SLAC-358
UC-403
(A)

SLAC SITE GEOLOGY, GROUND MOTION AND SOME EFFECTS OF THE OCTOBER 17, 1989 EARTHQUAKE

G. E. Fischer

Stanford Linear Accelerator Center
Stanford University
Stanford, California 94309

December 1989

Prepared for the Department of Energy
under contract number DE-AC03-76SF00515

Printed in the United States of America. Available from the National Technical Information Service, U.S. Department of Commerce, 5285 Port Royal Road, Springfield, Virginia 22161. Price: Printed Copy A04, Microfiche A01.

TABLE OF CONTENTS

APPENDICES

SLAC SITE GEOLOGY, GROUND MOTION AND SOME EFFECTS OF THE OCTOBER 17, 1989 EARTHQUAKE

G. E. FISCHER

December 1989

ABSTRACT

An attempt is made to correlate ground motions resulting from the October 17, 1989 (Loma Prieta) earthquake with the geologic features of the SLAC site. Recent deformations of the linac are also related to slow motions observed over the past 20 years. Measured characteristics of the earthquake are listed. Some effects on machine components and detectors are noted. Some recommendations regarding instrument site are made.

In carrying out this work it was necessary to find and review many of the original records which describe the site and which are still available today. Since only a portion of this material can be found in the published literature, a listing and location file of some of the relevant material is provided.

1. INTRODUCTION

The original builders of the Stanford Linear Accelerator Center (SLAC) payed a great deal of attention to questions of site suitability. At that time (early 1960s), before steering and focusing was introduced along the linac, it was then believed that the accelerator should remain aligned along a straight line ranging from within 0.06 inches in 250 ft to 1 inch in 10,000 ft for periods up to one year and 5 inches for "as long as possible."[1] The proximity of the San Andreas fault system has been commented on at length, but every responsible geologist then, as now, has stated that although earthquakes, and more interestingly their effects, cannot be predicted with accuracy, *"it is most unlikely that the accelerator tunnel will be damaged unless it crosses a fault which ruptures or is* *located within a zone of 'maximum intensity' or in terrain with potentially unstable topography and/or incompetent rock."* We shall see that this belief has been borne out at SLAC up to, and including, the recent past.

2 SLAC SITE GEOLOGY

2.1 General Features

The excavation for the housing for the two-mile long linear accelerator afforded geologists the best exposed cross section of Cenozoic (an age, including the present, during which mammals developed) rocks between the San Andreas fault and San Francisco Bay. The geology and physical properties of the site were studied during 1961–64 in an elaborate program of geologic mapping, boring, trenching, soil testing, and measurement of ground movement.

The geological aspects of this work are described by Benjamin Page and Larry Tabor.[2] Figure 1 is a reproduction of Plate 1 of their publication. The cross section shows "orderly Eocene sandstone, mudstone sequences interrupted by chaotic zones consisting of disordered mudstone with scattered and rotated bodies of sandstone." It is believed that the chaotic structure resulted in part from Eocene submarine sliding [although thrusting of the San Andreas fault system, had it been active in Eocene times ($>$ 50 MY), provides an alternative explanation]. After the Eocene rocks were moderately folded, Miocene ($\approx$ 10 MY) strata were deposited uncomformably upon them. Continued thrusting and folding produced a surface of décollement which itself increased the structural complexity of the chaotic zones, in places producing locally overturned intact strata. Such a hypothetical process is shown in a reproduction of their figure 4 (figure 2 of this report). These authors also single out a shallow "bedding plane fault" shown in their figure 5 (figure 3 of this report) between the Miocene deposits and the much more recent poorly consolidated fluvial conglomerate (Plio-Pleistocene age, $\approx$ 1 MY) named Santa Clara Formation by Prof. Branner at the turn of the century. This 10-ft-thick layer of sheared mudstone intersects the accelerator tunnel around Station 91+00 and played a part in recent events. Figure 4 is a photograph of the fault taken in 1964.

2.2 Geologic Details along the Linac Tunnel and in the Target Area

The above mentioned publication concerns itself primarily with the geologic structure of the site. The very detailed work on which it is based was carried out by Tabor and others for the architect, engineering and construction management firm Aetron-Blume-Atkinson (ABA). These investigations are contained in the massive report ABA-88.[3]

Figure 5 is a reproduction of Plate II of this report. It depicts the bedrock geologic cross section on which the linac tunnel is built. Since the defined elevations[4] of the tunnel floor are 297.300 ft at Station[5] 00+00 at the west end, and 247.300 ft at station 100+00 near the beginning of the beam switchyard, it is evident when one draws a line through these elevations on figure 5 that the tunnel rests on two "cut" and two "fill" regions. This fact will dominate most discussions regarding vertical tunnel movement. It is also significant that the cuts shave off the chaotic Eocene anticline protrusions in regions having approximate station coordinates 00+00 to 20+10 and 70+50 to 80+60. Fill, consisting of engineered and specially compacted material, is placed to elevate the so-called "broad valley syncline" (50+50 to 70+00) and the region from 30+70 to 40+90.

Figure 6 is a reproduction of Plate IIA, the plan view of the geologic map. This map did not accompany the original report in March 1965, but was distributed on November 16 of that year. The words *probable major fault zone* must have caused some measure of concern for it prompted the then technical director of ABA to issue a letter on December 16 explaining that this term "... means that in these areas there were zones of earth movement in the distant geologic past but there has been no discernible movement in historic time..." The reader may note by looking for the small "f" symbols on the drawings, that there appear to be no less than ten such faults crossing the tunnel. They occur at the demarcations of regions of differing species of rock.

Report ABA-88 also contains nine high-detail maps along the accelerator tunnel. Figures 7 and 8 are reproductions of portions of Maps 3+4 and 9, which are singled out for later reference.

A truly exhaustive program of earth movement studies was carried out starting in 1961, and resulted in a massive report[6] in 1966. The happy conclusion reached was that whatever consistent vertical or horizontal movements could be detected by the best conventional means at that time, they were *small and well within the limits of surveying accuracy and accelerator design tolerances.* The report also points out that measurements of rebound and of fill compaction were within calculated limits (i.e., 1 to 2 inches). The report is nevertheless of some interest since it indicates what limits could be placed on the problem at that time, and that tectonic deformation of the site was *not* found. The report also contains a description of the inverted pendulum system and lists the coordinates of all bench marks used.

2.3 Geologic Detail for the Construction of the PEP Tunnel

The earlier history of geologic investigations regarding the PEP site is described by Bob Gould.[7] The work done by Tabor, Earth Sciences Associates of Palo Alto, and the results of an intensive Summer 1975 drilling program are chronicled. Among the various problems that were described, the situation in PEP-Region 11 is noteworthy today. Lenses of siltstone in clay matrix were found in the Miocene of borehole 11-1. Slickensided surfaces and scaly clay were abundant throughout the 10-ft thickness of this material. The origin of this expansive matter is speculated on by M. Dalrymple.[8]

The detailed geotechnical report for the architect-engineering firm of PBQ&D, Inc./ Kaiser Engineers for PEP construction was written by the firm Dames and Moore.[9] On page 13 there is a description of the suspect region beginning with: "A very plastic claystone unit is present as an interbed in the vicinity of Station 19+00 as illustrated on Plate 2. The rock is characterized by a tendency to swell and demonstrates a loss of strength with time when unconfined and exposed to water" and ending with: "special tunnel design and construction should be applied in this vicinity."Figure 9 is a reproduction of Plate 2 (of 8 plates) from this report which provides high detail of the PEP bedrock geology. Note borehole PEP 11-4.

2.4 Geologic Investigations of the SLC Site

The preliminary site investigation for the SLC Arc tunnels and experimental hall was carried out by the firm of Dames and Moore.[10] This work was superseded when the collider hall and Arcs were sited much further upstream (west) by Earth Science

Associates (ESA) under subcontract to the A and E firm for the SLC, the Tudor Engineering Company of San Francisco. ESA's completed Title I Report was issued September 1982[11] and was in turn superseded by the Title II Report of July 1983.[12] Although the Title II report contains the logs from boreholes SLC 10 to SLC 24 one must enter the contract drawings[13] for the construction of the north and south tunnels to find the map which describes where these holes are located. Figure 10 is a reproduction of Plate 2 of the latter report, which shows the locations of all the bore holes, trenches and seismic refraction lines for the SLC. The "final" tunnel route is indicated. One may note (at about 9:30 o'clock on this route) the entry "strike slip movement" indicating a fault first identified by Tabor in the early 1960s on Map 9 (target area) in ABA-88. This fault, described as a "pinch and swell structure containing gaugy dark grey-blue clay with slikensides," can still be seen with the naked eye in the cut of the road to SPEAR, as a marked indentation in the grass just under SSRL Building No. 288. It is also identified on ESA Title I, figure 2 (figure 11 of this report). This figure also shows the clay lens found in PEP bore holes 11-1 and 11-4 projected to the SLC tunnel. The possibility of this lens causing mischief during SLC tunneling must have given rise to the drilling of SLC-12. When no clay was found (see ESA Title II report), this possibility was removed and is therefore not shown on the geologic contract drawing (figures 12 and 13 of this report). We will refer to all this detail later. Figures 14 and 15 depict other places in the SLC tunnels that have "interesting" geology.

3. PAST OBSERVATIONS OF GROUND MOTIONS

3.1 Cumulative Motion, 1966–1983

The SLAC laser alignment system[14] has been used since 1966 to measure transverse displacement of the linac with respect to a line drawn through two (more or less arbitrarily defined) reference positions (which may themselves be moving with time). Each linac sector (there are 30 in 10,000 ft) generally consists of eight 40-ft support girders, each of which houses a lens station. There are, therefore (including a number of auxiliary stations), almost 300 lens positions that can be monitored along the 2 mile stretch.

Figure 16 depicts the cumulative motion of the tunnel (defined to be negative of cumulative corrections applied to keep the linac straight) between the years 1966 and 1983. For historical reasons the ordinate is plotted in units of 0.001 inches, the abscissa is plotted in "station number" in which, for example, sector 22, girder 5, would be plotted as station 225. For the vertical scale, positive values mean up. For the horizontal scale, positive values mean motion to the south! If one looks at the data on a year- by-year basis (shown in subsequent figures), it is interesting to note that, on the average, the motion is nearly always in the direction it took in earlier years.

3.2 Correlation of Motion with Geology (Gould, 1968; Tabor, 1973)

Figure 17 depicts what appears to be the first quantitative correlation of the initial ground motion with site geology[15] by Bob Gould.

A similar study using a different base drawing is shown in figure 18; it appears to be in Tabors handwriting and carries the data to 1973. It emphasizes the cut and fill nature of the tunnel by plotting elevation relative to the tunnel floor.

The salient features are easy to see:

- The tunnel sags in regions of fill, even though preloads had been applied. However, the long-term settlement magnitudes are much smaller (1/4 inch) than the short-term values that were predicted[16] (1 to 2 inches).
- The tunnel heaves up in those regions where the soil was excavated. Even though these regions coincide with the cutoff peaks of chaotic Eocene, it was felt that this motion could be attributed to *rebound.*
- With a few exceptions there appears to be *no clear cut* correlation of the motion with any of the of the numerous terrain discontinuities labelled as "inactive faults."
- A sharp discontinuity (vertical and horizontal) occurs at station 12-3.
- A smaller discontinuity is evident in the end of sector 27 (see figure 18).

3.3 Difficulties with Linac Station 12-3.

The suggested most probable cause of this movement was "intermittent creep in a southerly direction of a 'chaotic' zone of material"[17] and the suggested most practical remedial action was to "remove some 15,000 to 20,000 cu. yds. of chaotic material above the klystron gallery level in the zone north of the affected area" to remove the gravity force of the hill. No mention was made of the "contact striking NW-SE" which crosses the accelerator at 12-3 (see figure 7 of this report). Subsequently (October 1968), 8,000 cu. yds. were removed and it was reported[18] that "there has been little or no apparent movement of 12-3, which may or may not be coincidental." Bulldozer activity verified the nature of the contact, hard on the west and very soft on the east. A groundwater level measurement program was initiated, which subsequently yielded the result that water levels were substantially (10 to 20 ft) higher on the north than on the south, indicating that the pea-gravel drain below the tunnel is plugged and the accelerator is acting like a water dam in this area. (Note: station 12-3 is still moving today!)

3.4 Correlation of Motion with Seasonal Groundwater Level Changes

By 1971 sufficient data had been accumulated to draw definite conclusions about the effect of groundwater levels in the "fill" area of sector 13. The seasonal correlations shown[19] in figure 19 are quite dramatic. Prof. Amos Nur goes on to state that such local deformations make the study of tectonic strain of the nearby San Andreas fault system somewhat difficult.

3.5 Difficulties with the "Test Lab Fault"

While there was no definitive effect on the accelerator alignment over the years at station 90+00 (sector 27-9), this fault nevertheless cracked the accelerator housing over a broad area, cracked the concrete floor of the klystron test lab, and can be seen in the cracks of the patio between the southeast corner of the A&E Building and the test lab. The location where the fault breaks the surface is shown in figure 6.

4. PROPERTIES OF THE OCTOBER 17, 1989 EARTHQUAKE

4.1 PARAMETERS

The parameters of this earthquake are displayed in figure 20.[20] About 20 miles of the San Andreas fault ruptured. The epicenter was 9 miles northeast of Santa Cruz at a depth of 11.5 miles. The linear accelerator is 32 miles from the epicenter. The magnitude is listed at 7.1 .

4.2 THE EVENT WAS FORECAST

By observing the long-term slip rate of a fault and dividing this value into the geodetically determined slip associated with the last major earthquake, one can—assuming linear behavior—calculate a return period for the event. The probability of such an event occurring in a given time is then simply the fraction of the time used up following the last time the event occurred. What makes this field of study so notoriously difficult is that the long-term slip rate and the effective slip are very difficult to measure. Moreover, values vary dramatically for various regions of ground along the fault. Nevertheless, the location and magnitude of the Loma Prieta event was fairly well forecast.[21] The role played by the Franciscan formation of the Black Mountain fault area (Upper Page Mill Road) is of particular interest to this locality since it appears to be a turning point of the San Andreas which divides the Peninsula into regions of higher (northern part, 2.5 meters and lower (southern part, 1 meter) regions of slip. The relevant paper[22] is reproduced as Appendix A.

4.3 ACCELEROMETER RECORD AT SLAC

Two self-triggering strong motion accelerometers were installed on the SLAC site in 1982. One instrument was placed in a special enclosure near the high survey tower located on the hill east of the research yard. This instrument[23] was meant to provide a free-field reading that is unencumbered by nearby manmade structures. A second instrument is housed in a locked wooden box located on the floor against the east wall of the high bay of the test lab (Building 044). This location was chosen to be right on top of the so called "test lab fault." Regrettably, the first instrument suffered water damage in 1988 and was removed from its enclosure by the USGS,[24] which provides service and which collects and analyzes the data. Figure 21 depicts the acceleration records from the test lab instrument. This data was corrected for instrumental response, digitized and integrated with respect to time to provide velocity and displacement values.[25] The record labeled 360 degrees is for the horizontal component; northerly positive. Two-hundred-seventy degrees denotes positive in the westerly direction. Peak recorded accelerations are 0.29 g north and 0.21 g west. Notice the peak dynamic amplitudes of 11 cm north and 9 cm west! The three largest horizontal displacement bumps are almost in phase and are along a SW/NE direction, coincidentally *parallel* to the direction of test lab fault. One may also note that, although the instruments cannot measure a DC component, there appears to have been more motion (slip?) to the west than to the east during the event.

4.4 Peak Accelerations Recorded vs. Distance from the Epicenter

Peak ground accelerations to be expected in an earthquake are of great importance in the design of earthquake-resisting structures.[26] Over the past two decades great strides have been made, not only in design but, as greater regions of California became better instrumented, also in a much better ability to separate two dominant variables in the problem; namely (a) local soil conditions, and (b) distance from the epicenter. Since the Loma Prieta event occurred almost in SLAC's backyard, it might be interesting to plot peak ground acceleration versus epicentral distance for this earthquake. Fortunately the data is readily available.[27] Figure 22 depicts the results, in which the square points denote maximum horizontal (either NS or EW accelerations observed, plotted as a fraction of the acceleration due to gravity "g." The reader may feel that the lower bound of this scatter plot is reasonably represented by the two curves of "rock" motion, as suggested by Blume for earthquakes of magnitude 7.0 and 7.25 for Miocene sandstone type of material. The scientific basis for such curves has been much advanced since 1960s. A recent work is by Joyner and Boore.[28] Some results of their work are explained in Appendix B.

In those cases in which the data exceeds "rock station" values, *the station was located on less competent ground.* Notice, in particular, the amplification for those stations in Bay mud. Such poor material is deemed responsible for the substantial damage that occurred in the Marina district of San Francisco (amplification as high as 15) and the collapse of I-880 structure in Oakland. Two stations are labeled as sitting on granite. Not surprisingly, they suffered accelerations less than those predicted by the curves.

Curves, such as are displayed on figure 22, should not be taken too seriously. They may be used as a design guide—*not* as a well founded predictions of what will happen in any given event, for several reasons. Among these reasons are the effects of local strata and those along the motions' flight path cannot be predicted in advance. Data from points having epicentral distances less than the length of the rupture are not only scarce, they are in the *near-field* of the radiating source.

Nevertheless, one cannot help but wonder why the acceleration measured by the instrument in the SLAC test lab is so high. Should we take this reading to be representative of what the accelerator housing or the SLC experimental pit (sited primarily on Miocene rock) were subjected to?

5. RECENTLY OBSERVED DISPLACEMENTS THOUGHT TO BE CAUSED BY THE EARTHQUAKE

5.1 LINAC

As luck would have it, a complete laser realignment of the linac had been carried out as recently as October 3, 1989, just two weeks prior to the event. Figure 23 depicts the difference between this data and that taken on October 25, 1989. The scales of the two graphs have been chosen to be identical. Comparing the data with that of figure (16), several features become evident:

- The pattern of downward displacements that occurred from the earthquake in the fill regions (in sectors 12, 13, 14, 18, and 19) is almost identical to the pattern of long-term motion.
- Similarly the pattern of vertical heave in sectors 24, 25, and 26 is identical to that observed in long-term motion. In magnitude the tunnel appears to have aged in 15 sec an amount approximately equivalent to 15 years!
- In contrast, very little motion (vertical or horizontal) is seen along the western end of the accelerator (sectors 0 through 11).

- The tunnel slipped approximately 7 mm to the north starting in the region between stations 28–1 and 28–5 or linac coordinates 90+00 and 91+62. One need hardly comment that this is just where the "test lab fault" crosses the accelerator housing. This motion was large enough that new cracks appeared in the housing wall and the main laser had to be repositioned. The chaotic zone (sectors 24, 25, and 26) slipped south by about 2 mm. We do not yet know where the remaining downstream portion of the BSY housing ended up. BSY laser alignment is scheduled to be performed in March.
- Lesser horizontal motions ($\approx$ 1 mm) occurred in the fill zones.

Realignment measures taken in November 1989 to restore the linac to immediate operation are described by Adolphsen et al.[29]

5.2 North SLC Arc

Figure 24(a) shows an apparent 12-mm horizontal discontinuity in the north SLC Arc magnets located just upstream of the north reverse-bend section. Survey teams were led to this point because the electron beam could not be transported past this region. Figure 24(b) shows that the magnets have also slipped vertically at this point. To check whether it was the floor that moved, rather than the magnet supports, a vertical check of floor rivets was performed. The results of this measurement are shown in figure 25. The break appears to occur at the entrance to achromat 8(a) at a point 1325 ft in the Arc "s" coordinate; i.e., from station linac 100+00 in the beam switchyard.

Although it is tempting to associate the north Arc discontinuity with the fault found by Tabor (see figures 11 and 12), the coordinates *do not match*. The fault is at 1100 to 1200 ft and the discontinuity occurs at 1325 ft. It is interesting to recall what the tunneling contractor said he found in this region: "Water encountered on April 26, 1984, makes the area between N 12+30 and 13+70 one of the wettest areas in the northwest tunnel."[30] According to the analysis of the Contract Inspectors Daily Reports on and around Day 199 (April 26, 1984), however, the muddy tunnel floor conditions were caused by "poor control of minor water inflows. A localized flow of 3 to 5 gpm was noted at station N 13+25, and moist-to-seeping ground was noted from N 13+70 to

12+50." Such flows were noted in other places, and there are no indications (in contrast to other problem areas, where swelling stone was encountered) in the inspectors logs of unusual geology.[31] With the exception noted at station 14+27 (set number 236) at which point a 3 ft x 4 ft x 14 inch piece of soft clay fell from the crown, "stand-up time" (i.e., unsupported integrity of the roof) is listed as good (greater than eight hours).

The authors interpretation of these facts are: The water probably runs along the clay lens found at PEP. This lens is oriented toward the SLC tunnel but does not intersect it (note borehole SLC 12). The earthquake moved the ground parallel to the slip plane of the lens and the nearby tunnel with it. This explanation appears plausible but no "smoking gun" has yet been found to substantiate the hypothesis. It is interesting to note that so far no other major discontinuities have appeared in the Arcs large enough to stop the beam. Certainly other regions possess more suspect geologies. Only a complete resurvey (apparently not warranted at this time) might detect such places.

5.3 PEP

A PEP elevation survey taken with the Hydrostatic Level System[32] is shown in figure 26. The values plotted represent changes with respect to the most recent data set taken prior to the earthquake in 1987. The deviations are large. Movements in prior years were generally at the rate of 1/2 to 1 mm/yr. One might expect some vertical weakness at locations where the PEP tunnel passes above the SLC tunnels. In the south this occurs almost in the middle of PEP IR-6 and is probably masked by the hall. On the north a dip is seen just west of IR-12 which coincides with the tunnel crossing. It is difficult to interpret the overall shape of the results except to note a pronounced discontinuity centered on IR-10. Interestingly, a discontinuity is also evident in the radial (horizontal) resurvey of the floor monuments shown in figure 27(a,b,c) at the same location; namely, halfway between IR-10 and the symmetry point of Arc 11. This is, of course, the location of the clay lens referred to in previous discussions.

6. MOTION OF EQUIPMENT RELATIVE TO THEIR HOUSING

In general, beam dynamics considerations dominate placement tolerances of components in the plane *transverse* to the particles' motion. For this reason great care is exercised in the mechanical design of the mountings to provide rigid, high resolution, and reproducible adjustments in this plane. Perhaps less attention is payed to constraints in the axial direction. Although vacuum integrity was nowhere compromised, we discuss in this section three areas in which the earthquake produced effects which may require more attention in the future.

6.1 The Linac Alignment System Light Pipe

The copper waveguide of the accelerator proper is supported on some 240 strongback girders, each 40-ft long consisting of 2-ft diameter hollow aluminum tube. These tubes are connected with each others ends by means of 24-inch diameter, 2-inch long vacuum bellows to permit their evacuation, while allowing for thermal expansion. Mounting to the floor and side wall of the tunnel is shown in figure 28. Axial restraint is by means of a brace per girder to the wall, as shown. The brace fasteners are held to unistruts imbedded in the wall by dogs that resist shear forces through friction. During the earthquake considerable longitudinal waves must have been set up in the structure, which has all the properties of a mechanical delay line. Judging by scrapes on the paint between the wall and mounts, amplitudes up to ± 0.75 inches appear to have occurred. Most stations moved between 1/8 inch and 1/4 inch. Eight sections did not return to their equilibrium positions. Vacuum bellows problems also occurred at the accelerating waveguide itself. Some 16 focusing magnets had to be opened to repair these problems.[33]

6.2 The Arc Magnets

Similar effects occurred in the mounts of the SLC Arc magnets. Some mounts were bent so as to move the magnets in the axial direction. In the Arcs the situation is aggravated by the fact that the tunnels are not in a horizontal plane, and in fact have slopes up to 10%. Axial motions up to 1/2-inch were sufficient to completely collapse some vacuum bellows. Abnormal conditions were observed in 13 places in south Arc achromats 4, 10, 11, 18, 20, 21, 22, and 23. Deformations were also observed in 36 locations of north Arc achromats 10, 11, 12, 13, 14, 15 and 16.

6.3 The MARK II Detector

The central portion of the 1800-ton MARK II detector is mounted on four specially designed "Seismic Base Isolators,"[34] so that it need not be fully braced to the experimental pit walls. Generic versions of the pads are described in figure 29. Since no damage appears to have been done to the MARK II detector, we infer that the mountings performed as designed. The question arises: With what amplitude did the 1800 tons move relative to the floor during the earthquake? This amplitude is a nonlinear function of the peak accelerations applied by the earthquake (see curves 3 and 4 of figure 29). Since we do not have a record of the *actual* acceleration of the collider hall floor, we can only set some limits. Let us assume the test lab recorded values obtained in the collider hall. From curve 3, figure 29, we obtain a force reduction to 60% for a maximum acceleration of 0.29 g. Lesser forces have lesser reductions. Making the drastic assumption that the frequency response is the same (probably unwarranted), one would guess that the MARK II had an maximum amplitude of about 6 cm. Was this possible? Probably not! The central vacuum chamber bellows would have taken up this amount of motion, but the bellows protector would have been damaged. Marks on the protector are consistent with only 1/2-inch motion.[35] After all the motion ceased, the detector came to rest about 0.4 inches south and 0.14 inches west from where it had been before the quake (see figure 30). The detector has since been realigned.

7. CONCLUSIONS

Although additional alignment information will continue to become available in the coming year, the following conclusions may be drawn at this time.

- Permanent deformations of the accelerator housing and Arc tunnels ($\approx$ 1 cm) appear to have occurred at sharp locations that have either known or suspected geologically recent *clay* formations.

- Other more broadly distributed deformations of the linac have occurred in regions that have been traditionally associated with sagging fill or rebound of cuts. The patterns of deformations are the same, the magnitudes (1 to 2 cm) are comparable to slow motions that have been accumulating since construction in the mid-1960s.
- No deformations appear to have occurred at faults which have been considered "geologically inactive."
- We *do not* have unambiguous evidence of what accelerations the experimental collider hall and the accelerator housing (in which some of the laboratory's most valuable equipment is located) were subjected to. One would therefore propose the relocation of the existing accelerometer to such locations, or the purchase and installation of additional instruments.
- Since the recent earthquake has served to *increase* the sum probability of an event in the Southern San Francisco Peninsula or along the Hayward fault in the East Bay to about 50% in the next 30 years, it would seem prudent to begin discussions of cost/benefit evaluations of further earthquake countermeasures over the projected lifetime of the facility. Axial restraints are an example that might be worth looking into.

ACKNOWLEDGMENTS

It is a pleasure to acknowledge the assistance rendered by many members of the SLAC staff and others in compiling this report. In particular, I wish to thank Bob Gould for providing advice and opening his files to me. Thanks to Bob Bell, Glenn Tenney, and Gordon Ratliff for helping to find reports and records; to Bob Laughead and Clay Corvin for permitting me to acquire the original SLC tunnel data; to Clyde Earnest, Tudor Engineering, San Francisco, CA, for help in interpreting this material; to Sean Deyer for providing the MARK II motion record; to Al Lisin and John Rees for their valuable comments, and above all to the SLAC Survey and Alignment Group under the direction of Robert Ruland for permitting the use of their recent alignment data in this report. I am indebted to Sylvia MacBride for her patience and understanding with respect to the graphics.

LOCATION OF RECORDS

The early geologic reports and other material from which information was extracted in compiling portions of this report may be entered by addressing the SLAC Archivist.[36]

REFERENCES

1. *Geological Investigation of the Stanford Two-Mile Linear Accelerator Site,* F. W. Atchley and R. O. Dobbs, *Microwave Laboratory Report No. 682,* January 1960, p. 1–14. (Note: Although this 150-page report discusses the so-called "tunnel" site parallel to Junipero Serra Blvd. which was later replaced, due to cheaper construction, by the "cut and cover" Sand Hill site, it nevertheless is relevant to our study because it lays the groundwork for further investigations. Introduced are Dames and Moore's first soils reports, Prof. Perry Byerly's comments on the regions seismicity and his notion of strain deformation of the site due to tectonic motion of the locked San Andreas fault. (pp. 3-18 to 3-23 and Appendix III).
2. *Chaotic Structure and Décollement in Cenozoic Rocks near Stanford University, CA,* B. M. Page and L. L. Tabor, *Geological Society of America Bulletin,* Vol. 78, p. 1–12, January 1967.
3. *Geologic Site Investigation for the Stanford Linear Accelerator Center,* Report No. ABA–88, March 1965, unpublished.
4. These elevations are for the Clark 1866 Spheroid with parameters listed in ABA Report 106, May 1966.
5. The *Z* coordinate system of the tunnel consists of station coordinates in which for example 00+00 is the starting point and 100+50 would be 10,050 ft in the direction of the beam.
6. *Earth Movement Investigations and Geodetic Control of the Stanford Linear Accelerator Center,* J. R. Brittain, J. R. Boyle, Report No. ABA-106, May 1966.
7. Geotechnical Investigations of the PEP Site, R. S. Gould, PEP–206, Feb. 1976.
8. Mark Dalrymple, PEP site test boring, letter to R. S. Gould, December 30, 1975.
9. *Geotechnical Investigation, Proposed Positron-Electron Project, SLAC, Stanford CA,* Dames and Moore, Job No. 0651-130, June 1, 1977.
10. *Preliminary Geological and Soils Site Investigation—Proposed Stanford Linear Collider (SLC)* Dames and Moore Job No. 10805–065–03, June 24, 1981.
11. *Title I Geotechnical Report for the SLAC–SLC North and South Arc Tunnels,* Earth Sciences Associates, 701 Welch Road, Palo Alto, CA 94304, Report G144, September 1982.

12. *Title II Geotechnical Report for the SLAC–SLC North and South Arc Tunnels,* Earth Sciences Associates, 701 Welch Road, Palo Alto, CA 94304, July 1983.

13. *Contract Drawings for the Construction of the SLC North and South Arc Tunnels,* Tudor Engineering, San Francisco (ID 372–030–01 through ID 372–030–10).

14. *Precision Alignment Using a System of Large Rectangular Fresnel Lenses,* W. B. Herrmannsfeldt et al., *Applied Optics,* **Vol. 7,** 995 (1968).

15. R. S. Gould, unpublished notes, 1968.

16. Dames and Moore, letter to ABA, January 29, 1964.

17. Roland Sharpe of John Blume Associates, San Francisco, letter to R. S. Gould, June 18, 1968.

18. Unsigned progress report, 1968.

19. *Seasonal Deformations of 2-Mile Straight Line,* J. J. Spranza, A. M. Nur, *Journal of the Soil, Mechanics and Foundations Division, Proc. of the American Society of Civil Engineers,* **Vol. 97, No. SM12,** December 1971, p. 1623.

20. *The Loma Prieta Earthquake of October 17,1989,* U.S. Geological Survey pamphlet P. L. Ward, R. A. Page et al., 1989.

21. *Probabilities of Large Earthquakes occurring in California on the San Andreas Fault,* The Working Group on California Earthquake Probabilities, USGS OFR–88–398, Menlo Park, 1988.

22. *The Black Mountain Asperity: Seismic Hazard of the Southern San Francisco Peninsula,* C. H. Scholz, Lamont-Doherty Geo. Obs., Columbia Univ., Paper 5L6649, American Geophysical Union, 1985.

23. Made by Kinemetrics in Southern California.

24. Mr. Edwin Etheredge, USGS, 345 Middlefield Rd., Menlo Park, CA 94025, (415) 329–5667.

25. These curves were made available through the courtesy of Dr. Gerald Brady, USGS, 345 Middlefield Rd., Menlo Park, CA 94025, (415) 329–5664.

26. See for example: John A. Blume, *Earthquake Design Considerations for the Accelerator Housing Structures of the Stanford Linear Accelerator Center,* Report No. 2, June 3, 1963, pp. 6–9.

27. Report No. 0SMS 89–06, Office of Strong Motion Studies, Division of Mines and Geology, California Department of Conservation, 630 Bercut Drive, Sacramento, CA 95814.

28. *Measurement, Characterization, and Prediction of Strong Ground Motion,* W. B. Joyner and D. M. Boore, *Proc. of Earthquake Engineering and Soil Dynamics II, GT Div./ASCE,* Park City, UT, June 27, 1988.

29. SLC Accelerator Physics Experiment No. 115, C. Adolphsen, F. Linker, W. Oren, R. Ruland, and J. Seeman, November 21, 1989.
30. Gates and Fox, Claim No .2, September 11, 1985, p. 33.
31. Clyde Earnest, Tudor Engineering, San Francisco, CA, December 1989, private communication.
32. T. Lauritzen and R. Sah, *IEEE Trans. Nucl. Sci.,* **Vol. NS–28, No. 3,** June 1981.
33. Letter from C. Perkins to L. Gianini, October 30, 1989.
34. Dynamic Isolation Systems, Inc., 2855 Telegraph Ave., Suite 410, Berkeley, CA 94705, (415) 843-7233.
35. Julia Weiler, SLAC Vacuum Group, January 1990, private communication.
36. Who may be found through the SLAC Library.

FIGURE CAPTIONS

1) Geologic map of the SLAC site (from Page and Tabor).
2) From Page and Tabor.
3) From Page and Tabor.
4) Photograph of the fault taken during construction, 1964.
5) Bedrock geologic cross section under linac, (reproduction of Plate II, ABA-88).
6) Plan View–Bedrock Geologic Map, (Plate IIA, ABA-88).
7) Reproduction of Map 3+4, ABA-88.
8) Reproduction of Map 9, ABA–88.
9) Reproduction of Plate 2 (of 8 plates) PEP bedrock geology.
10) Plate 2: Contract construction drawings for SLC Arc tunnels.
11) From Earth Sciences Title I Report.
12) From SLC Arc tunnel construction contract drawings, station 0 to N 12+00.
13) From SLC Arc tunnel construction contract drawings N 12+00 to N 22+00.
14) From SLC Arc tunnel contract drawings N 24+00 to N 34+00.
15) From SLC Arc tunnel contract drawings S 37+00 to S 47+00.
16) Cumulative linac tunnel displacements between 1966–1983.
17) Correlation of Ground Motion with Site Geology, R. S. Gould, 1968.
18) Study by L. Tabor, 1973.
19) Seasonal motions correlated with rainfall and ground water levels (from Spranza and Nur, 1971).

20) Parameters of the Loma Prieta Earthquake, (from USGS).

21) Records of corrected acceleration, velocity, and displacement from the instrument located in the test lab. Courtesy USGS, Menlo Park.

22) Measured maximum horizontal ground accelerations vs. distance from the epicenter.

23) Displacement of linac tunnel between October 3 and 25, 1989.

24) Horizontal and vertical discontinuities in north SLC Arc in achromat 8(a).

25) Vertical survey of floor elevation rivets near achromat 8.

26) Hydrostatic Level survey of the PEP tunnel, 1987 to December 1989.

27) Horizontal survey of PEP floor monuments, December 1989.

28) Method of support—Linac Girder.

29) Brochure describing commercially available earthquake isolation systems, from DIS, Inc., Berkeley, CA.

30) Change in location of MARK II detector due to earthquake.

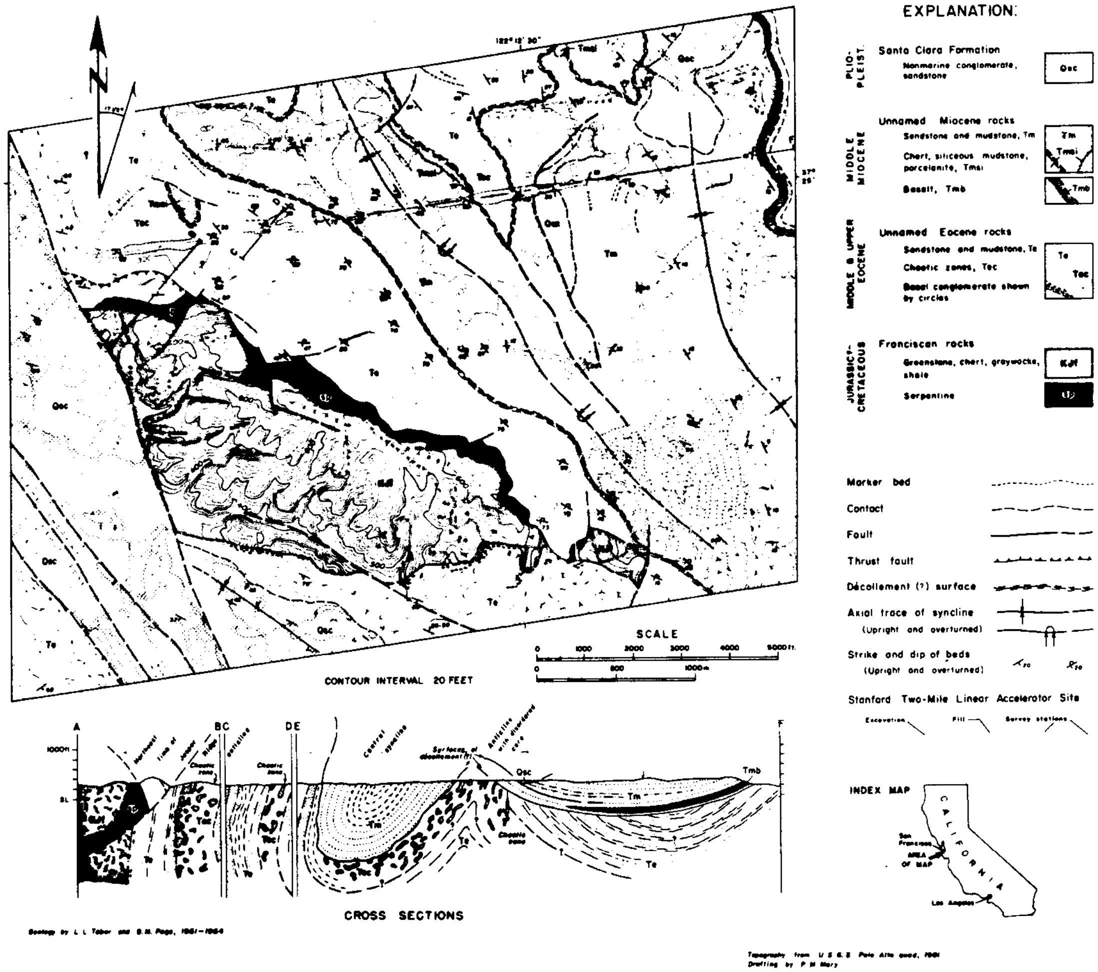

GEOLOGIC MAP OF AREA WEST OF STANFORD UNIVERSITY, CALIFORNIA

Geology by Page and Tabor, 1961–1964; topography from U.S. Geological Survey Palo Alto quadrangle, 1961; drafting by P. M. Mary

PAGE AND TABOR, PLATE 1
Geological Society of America Bulletin, volume 78

6565B1

Fig. 1

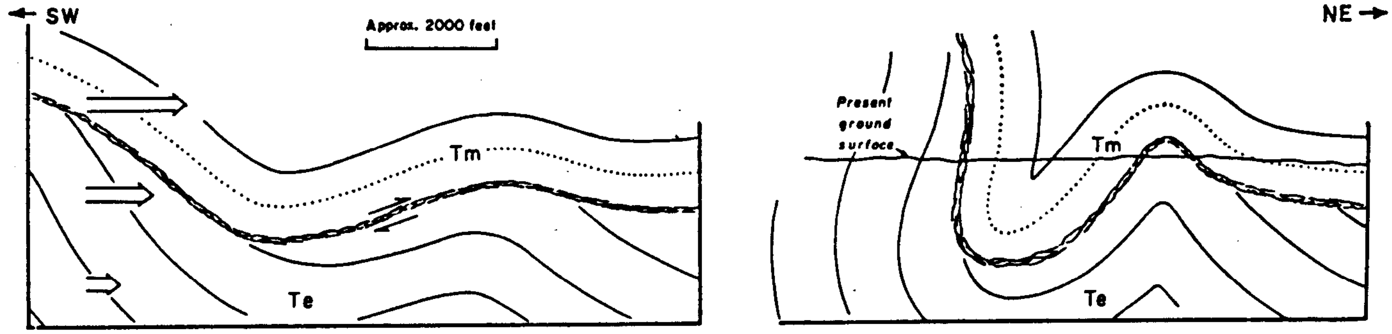

Figure 4. Hypothetical development of décollement between Miocene and Eocene rocks, Stanford, California. Miocene rocks (Tm) moved to right relative to Eocene rocks (Te). Eventually décollement surface was strongly folded (right). Santa Clara Formation is not shown; it would overlie "Tm."

6565A2

Fig. 2

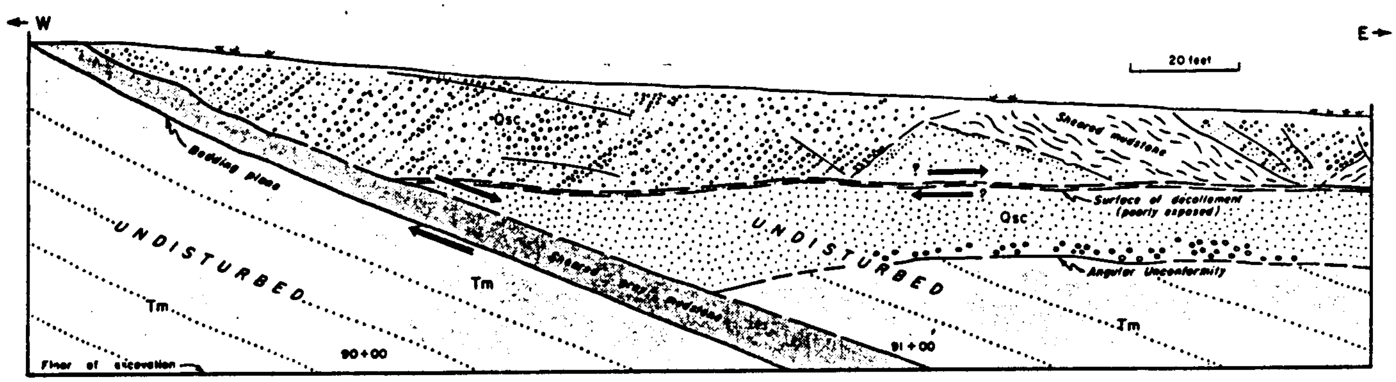

Figure 5. Décollement involving Pliocene-Pleistocene rocks. Horizontal conglomerate of Santa Clara Formation (Qsc) rests unconformably on Miocene beds (Tm). Tilted and jumbled Santa Clara beds have slid on ill-defined décollement surface. Fault parallel with Miocene beds has offset earlier structures. (Side of linear accelerator excavation near station 91+00. View has been reversed from actual exposure, so observer is looking in about the same direction as in Figure 4. Vertical scale is same as horizontal scale.)

6565A3

Fig. 3

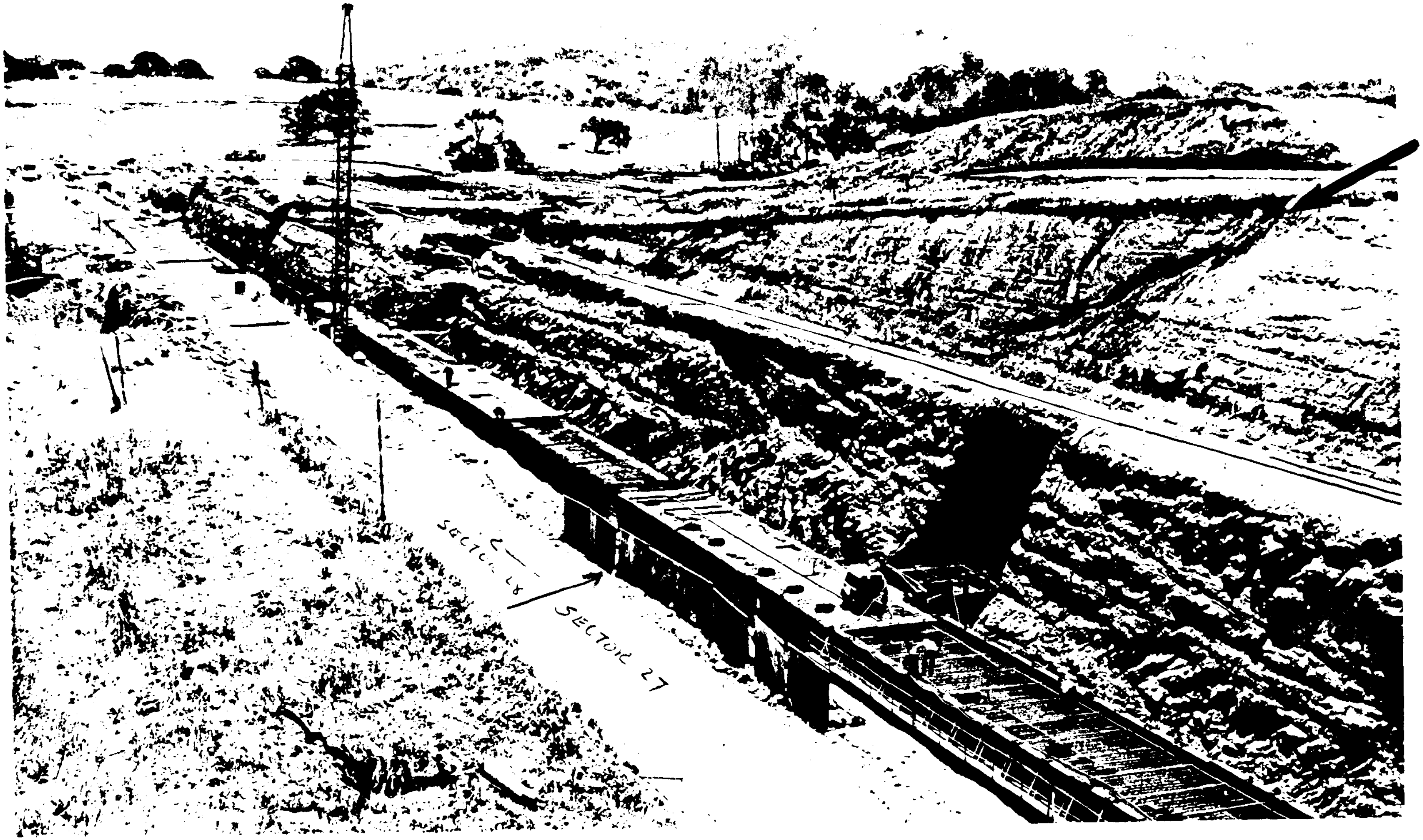

6565A4

Fig. 4

JUN 12 '64

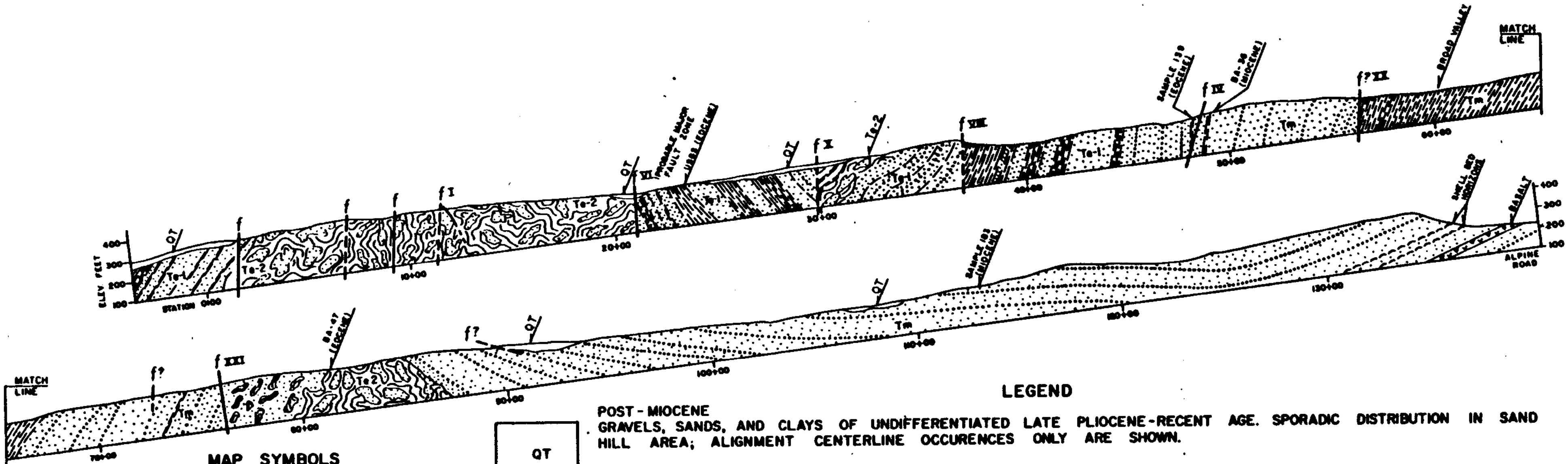

MAP SYMBOLS

- NORMAL CONTACT (INFERRED)
- FAULTS (KNOWN & INFERRED)
- 48 STRIKE & DIP
- 48 OVERTURNED STRATA
- AXIS OF ANTICLINE
- AXIS OF SYNCLINE
- 343 PALEONTOLOGICAL SAMPLE (SURFACE)
- BA-48 PALEONTOLOGICAL SAMPLE (SUBSURFACE) (BOREHOLE FROM WHICH TAKEN)

LEGEND

QT	POST-MIOCENE GRAVELS, SANDS, AND CLAYS OF UNDIFFERENTIATED LATE PLIOCENE-RECENT AGE. SPORADIC DISTRIBUTION IN SAND HILL AREA; ALIGNMENT CENTERLINE OCCURENCES ONLY ARE SHOWN.
Tm	MIOCENE LIGHT COLORED, WELL SORTED SANDSTONES AND SILTSTONE; DARK COLORED CLAYSTONES, STRATIGRAPIC POSITION UNKNOWN, IN BROAD VALLEY. INTERBEDDED SHELL-FRAGMENT SANDSTONES AND BASALT FLOW, NEAR BASE, IN ALPINE ROAD LOCALITY.
Te (Te-2, Te-1)	EOCENE LIGHT TO DARK COLORED, ILL-SORTED SANDSTONES AND INTERBEDDED DARK COLORED CLAYSTONES AND SILTSTONES OF NORMAL DEPOSITION (Te-1), AND ASSOCIATED CHAOS ROCKS (Te-2), DERIVED FROM Te-1 ROCKS. CHAOS ROCKS SHOWN ONLY ON STRUCTURAL SECTION.
Jsp	JURASSIC (?) PRINCIPALLY SERPENTINE; ASSOCIATED SCHIST AND FRANCISCAN (?) SANDSTONE IN LOWER PART OF BEAR CREEK.

6565B5 ASTON-BLUME-ATKINSON

BEDROCK GEOLOGIC MAP OF STANFORD LINEAR ACCELERATOR CENTER

PLATE II

Fig. 5

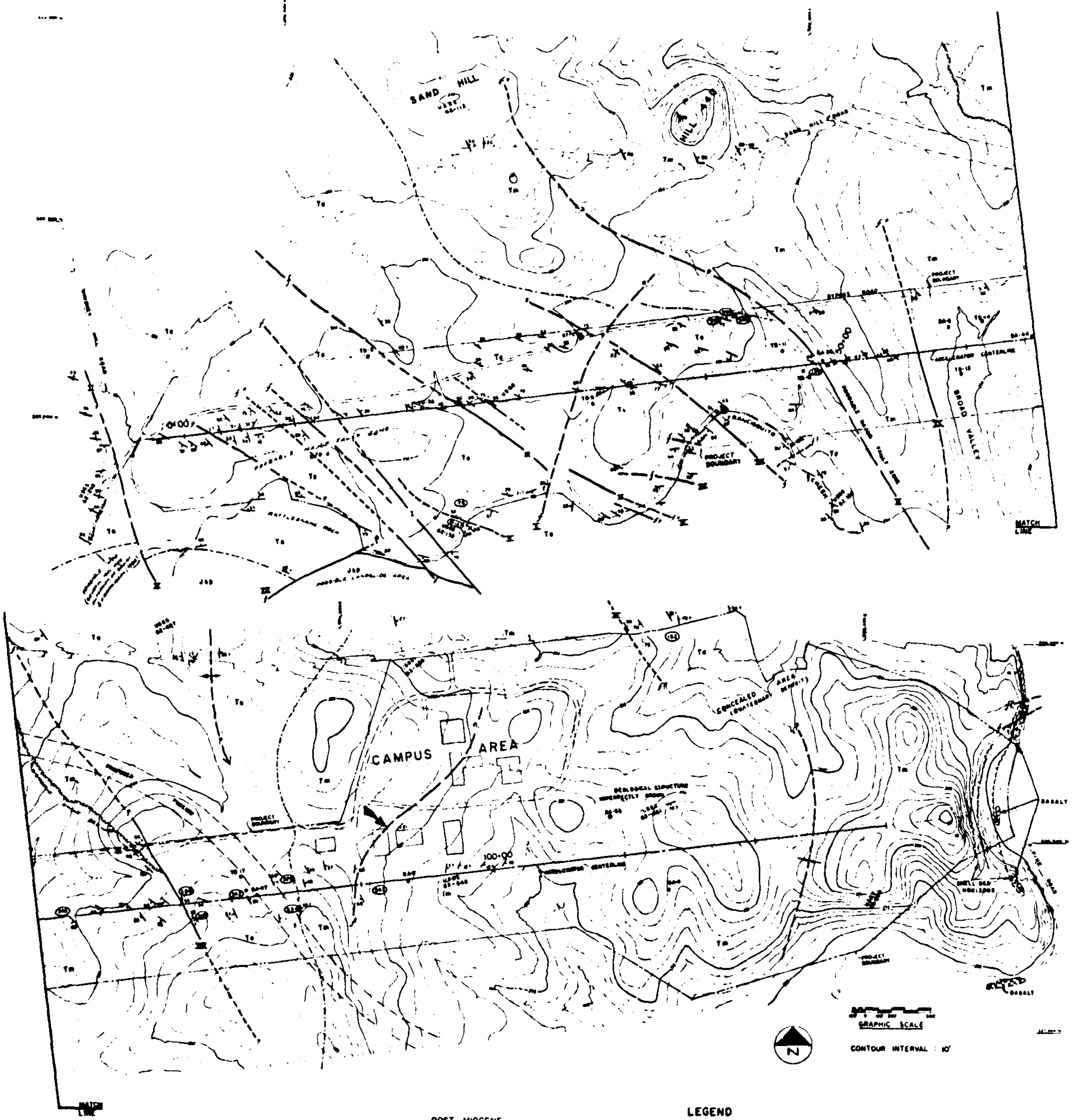

MAP SYMBOLS

	NORMAL CONTACT (INFERRED)
	FAULTS (KNOWN & INFERRED)
46	STRIKE & DIP
48	OVERTURNED STRATA
	AXIS OF ANTICLINE
	AXIS OF SYNCLINE
343	PALEONTOLOGICAL SAMPLE (SURFACE)
BA-48	PALEONTOLOGICAL SAMPLE (SUBSURFACE) (BOREHOLE FROM WHICH TAKEN)

LEGEND

QT	POST - MIOCENE GRAVELS, SANDS, AND CLAYS OF UNDIFFERENTIATED LATE PLIOCENE-RECENT AGE. SPORADIC DISTRIBUTION IN SAND HILL AREA, ALIGNMENT CENTERLINE OCCURENCES ONLY ARE SHOWN.
Tm	MIOCENE LIGHT COLORED, WELL SORTED SANDSTONES AND SILTSTONE; DARK COLORED CLAYSTONES, STRATIGRAPIC POSITION UNKNOWN, IN BROAD VALLEY. INTERBEDDED SHELL-FRAGMENT SANDSTONES AND BASALT FLOW, NEAR BASE, IN ALPINE ROAD LOCALITY.
Te (Te-2, Te-1)	EOCENE LIGHT TO DARK COLORED, ILL-SORTED SANDSTONES AND INTERBEDDED DARK COLORED CLAYSTONES AND SILTSTONES OF NORMAL DEPOSITION (Te-1), AND ASSOCIATED CHAOS ROCKS (Te-2), DERIVED FROM Te-1 ROCKS. CHAOS ROCKS SHOWN ONLY ON STRUCTURAL SECTION.
Jsp	JURASSIC (?) PRINCIPALLY SERPENTINE; ASSOCIATED SCHIST AND FRANCISCAN (?) SANDSTONE IN LOWER PART OF BEAR CREEK

ASTRON-BLUME-ATKINSON

6665C6

BEDROCK GEOLOGIC MAP OF STANFORD LINEAR ACCELERATOR CENTER

PLATE II A

Fig. 6

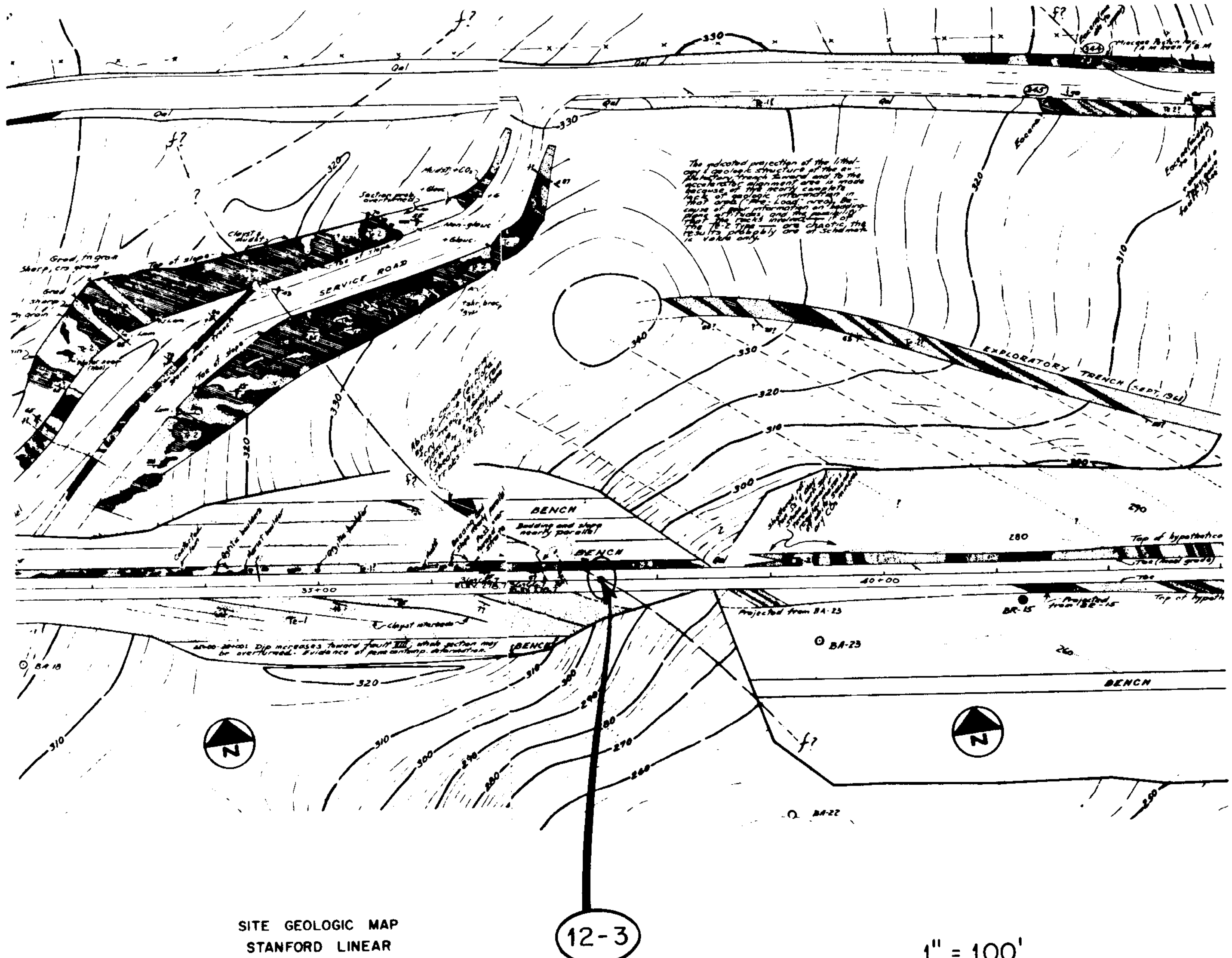

SITE GEOLOGIC MAP
STANFORD LINEAR
ACCELERATOR CENTER
MAP 3 STATION 23+33.3 TO STATION 36+66.7

1" = 100'

6565A7

Fig. 7

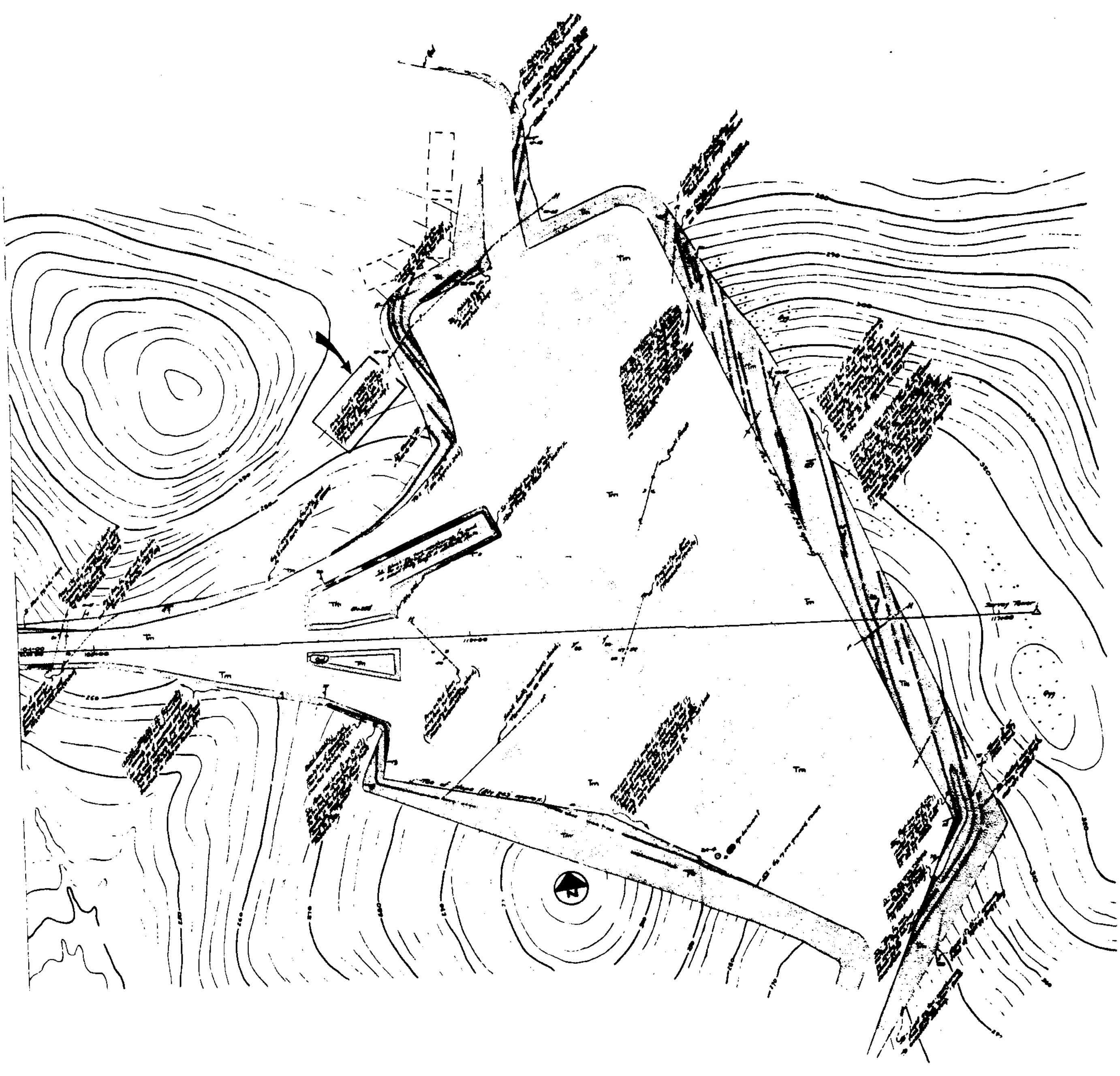

SITE GEOLOGIC MAP
STANFORD LINEAR
ACCELERATOR CENTER
MAP 9 STATION 104+00 TO STATION 117+50

6565C8

Fig. 8

AETRON-BLUME-ATKINSON

[redacted]

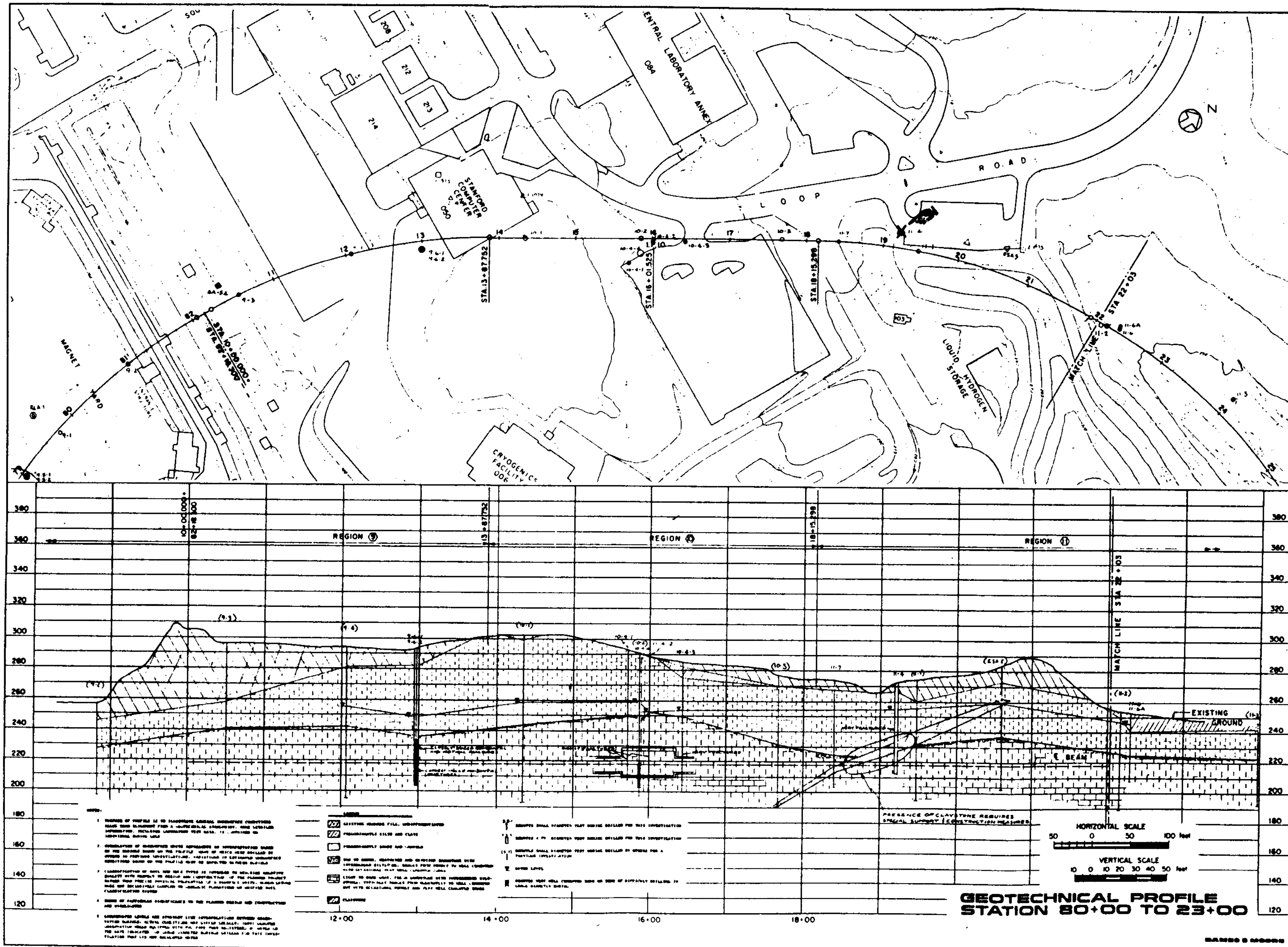

Fig. 9

6565B9

PLATE 2

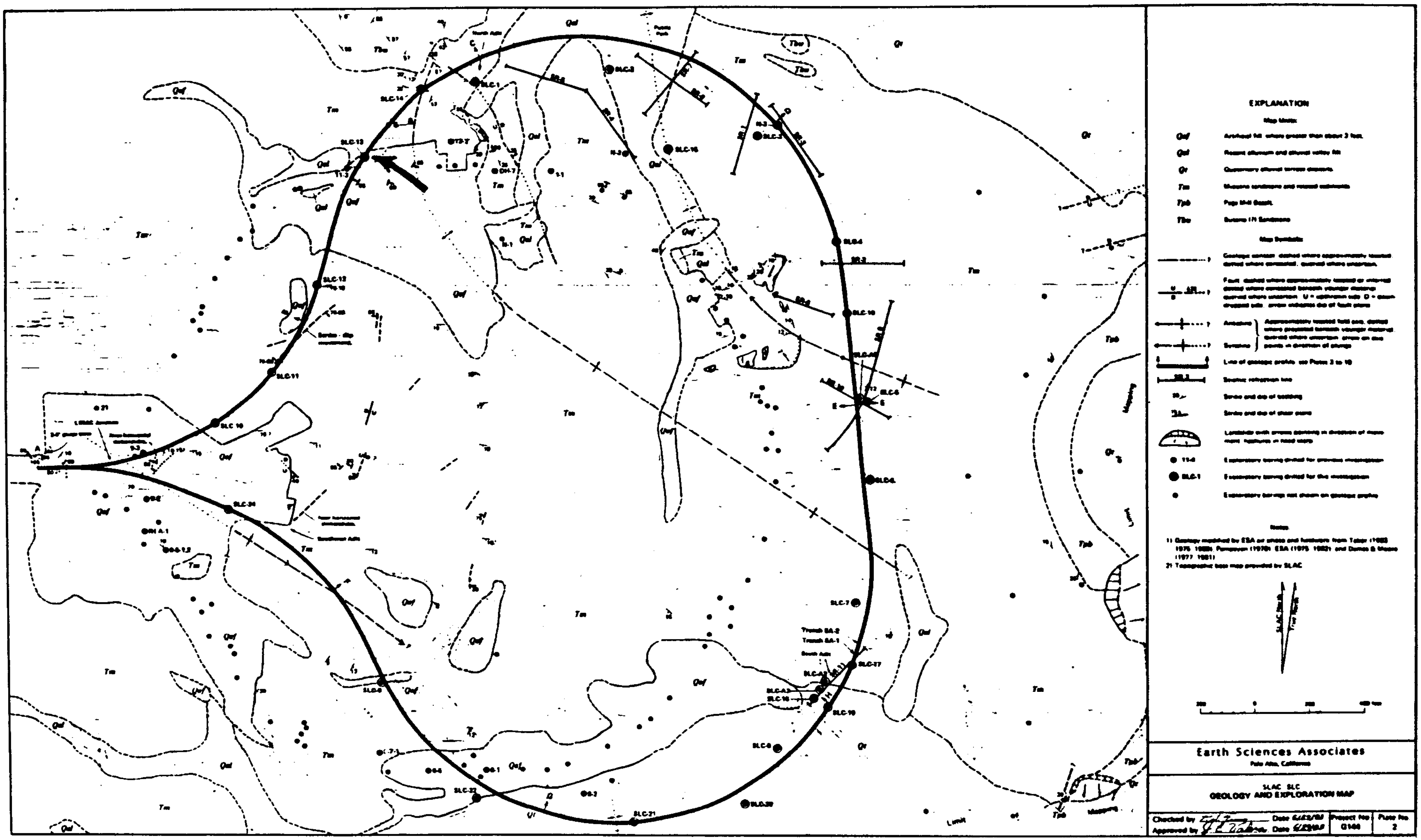

6565A10

Fig. 10

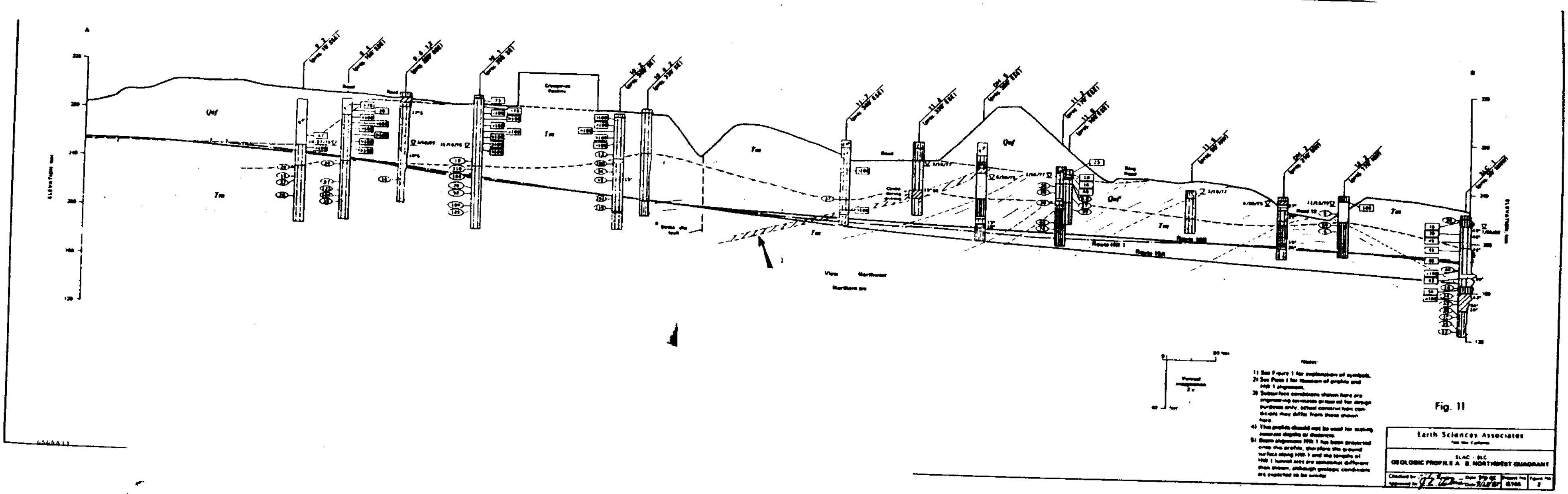

Qaf
Tm
Route HW 1
View Northwest
Vertical exaggeration 2 x
Notes
1) See Figure 1 for explanation of symbols.
2) See Plate 1 for location of profile and HW 1 alignment.
3) Subsurface conditions shown here are engineering estimates prepared for design purposes only, actual construction conditions may differ from those shown here.
4) This profile should not be used for scaling accurate depths or distances.
5) Beam alignment HW 1 has been projected onto this profile, therefore the ground surface along HW 1 and the lengths of HW 1 tunnel arcs are somewhat different than shown, although geologic conditions are expected to be similar.
Earth Sciences Associates
SLAC - SLC
GEOLOGIC PROFILE A B NORTHWEST QUADRANT
Checked by
Approved by
Date
Project No
Figure No
2

Fig. 11

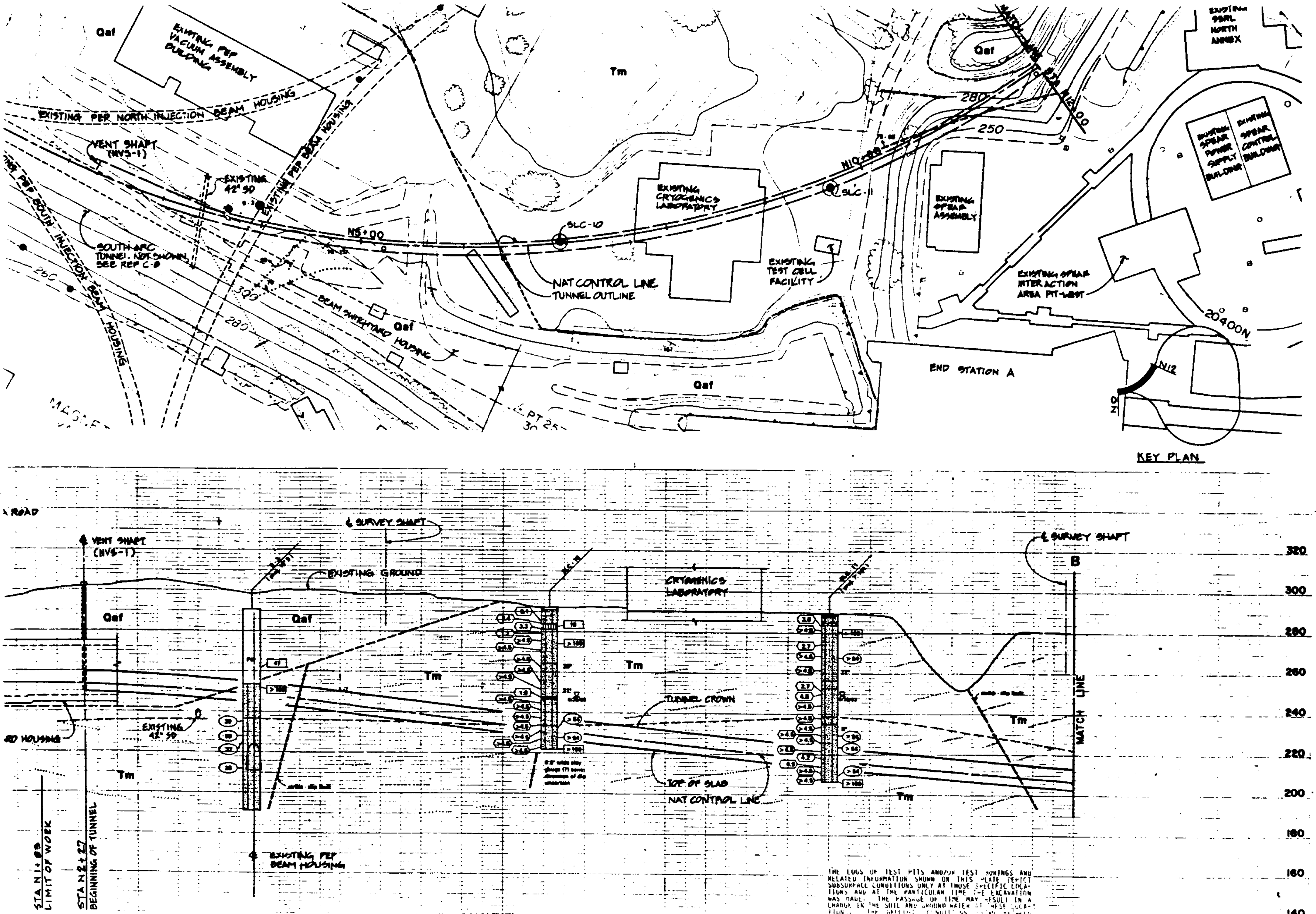

Fig. 12

6565A1

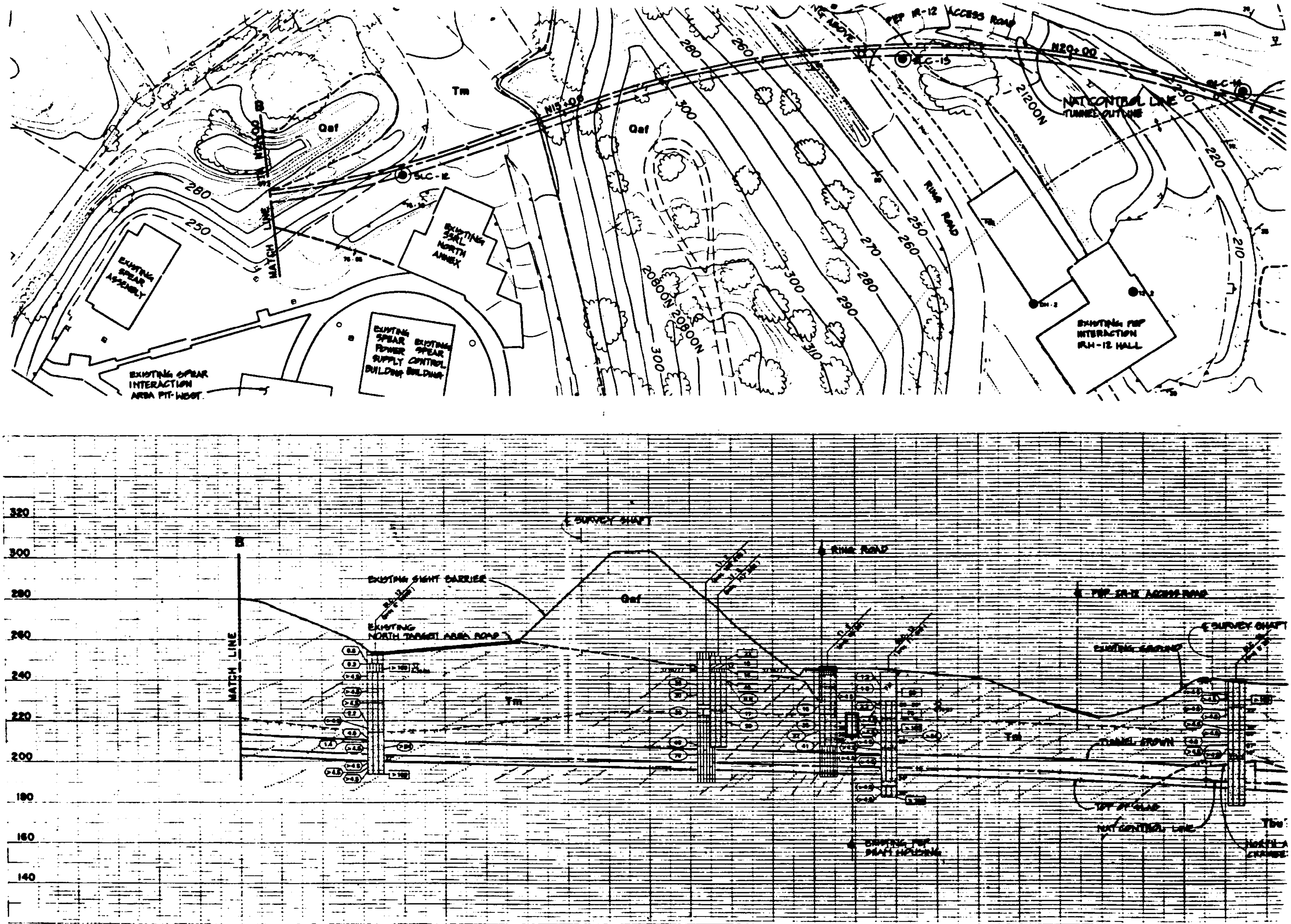

Fig. 13

6565A13

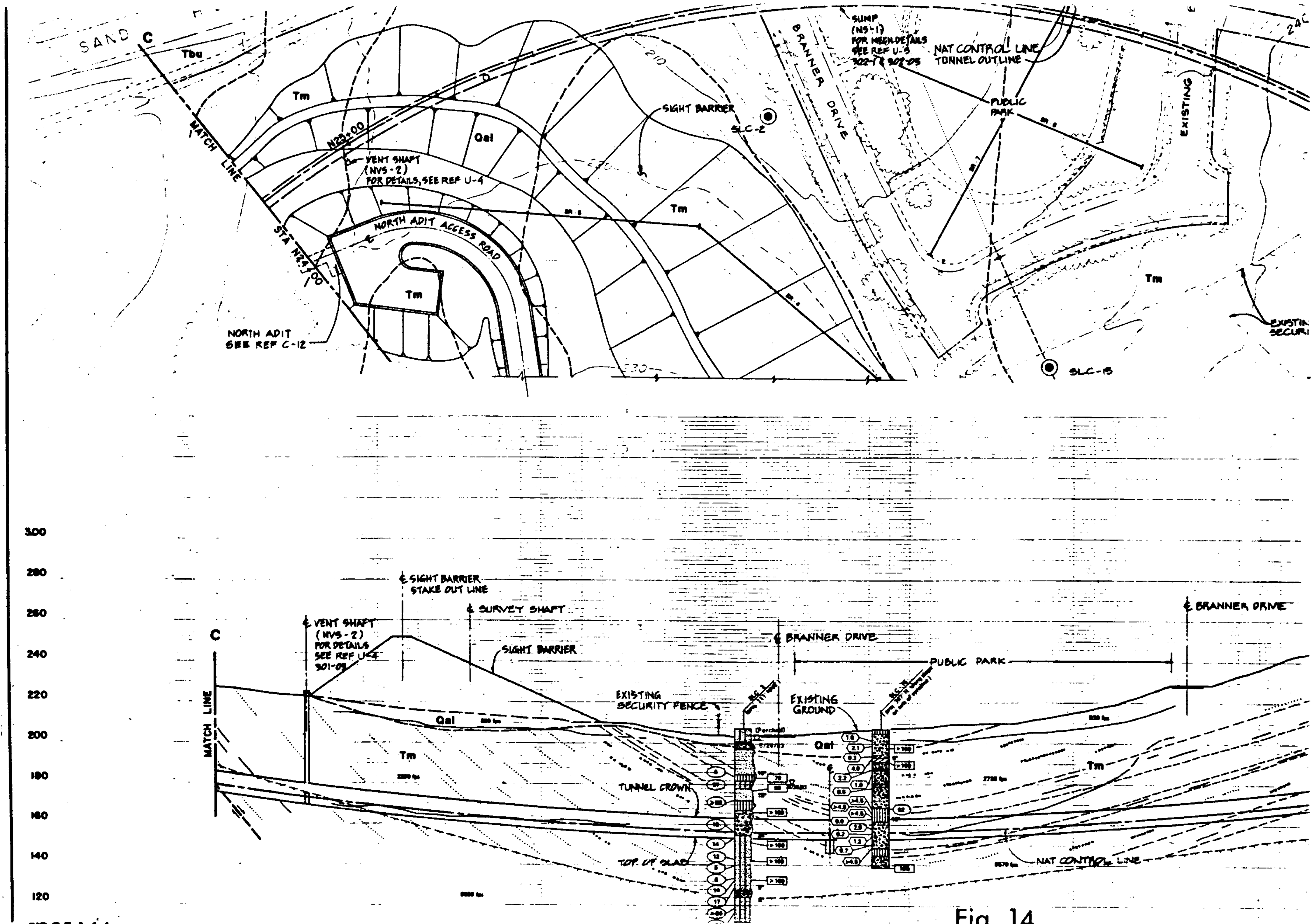

6565A14

Fig. 14

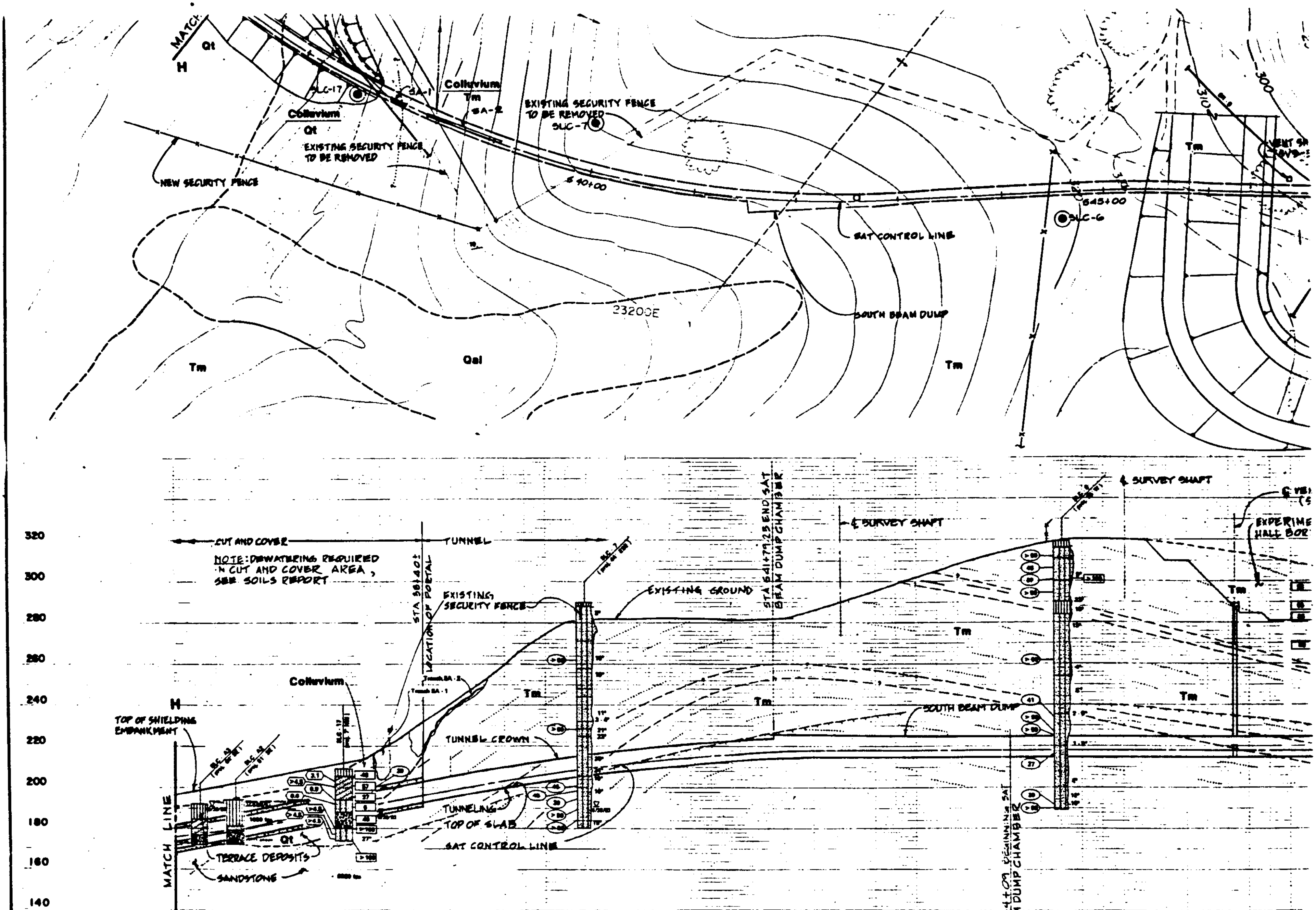

Fig. 15

6565A15

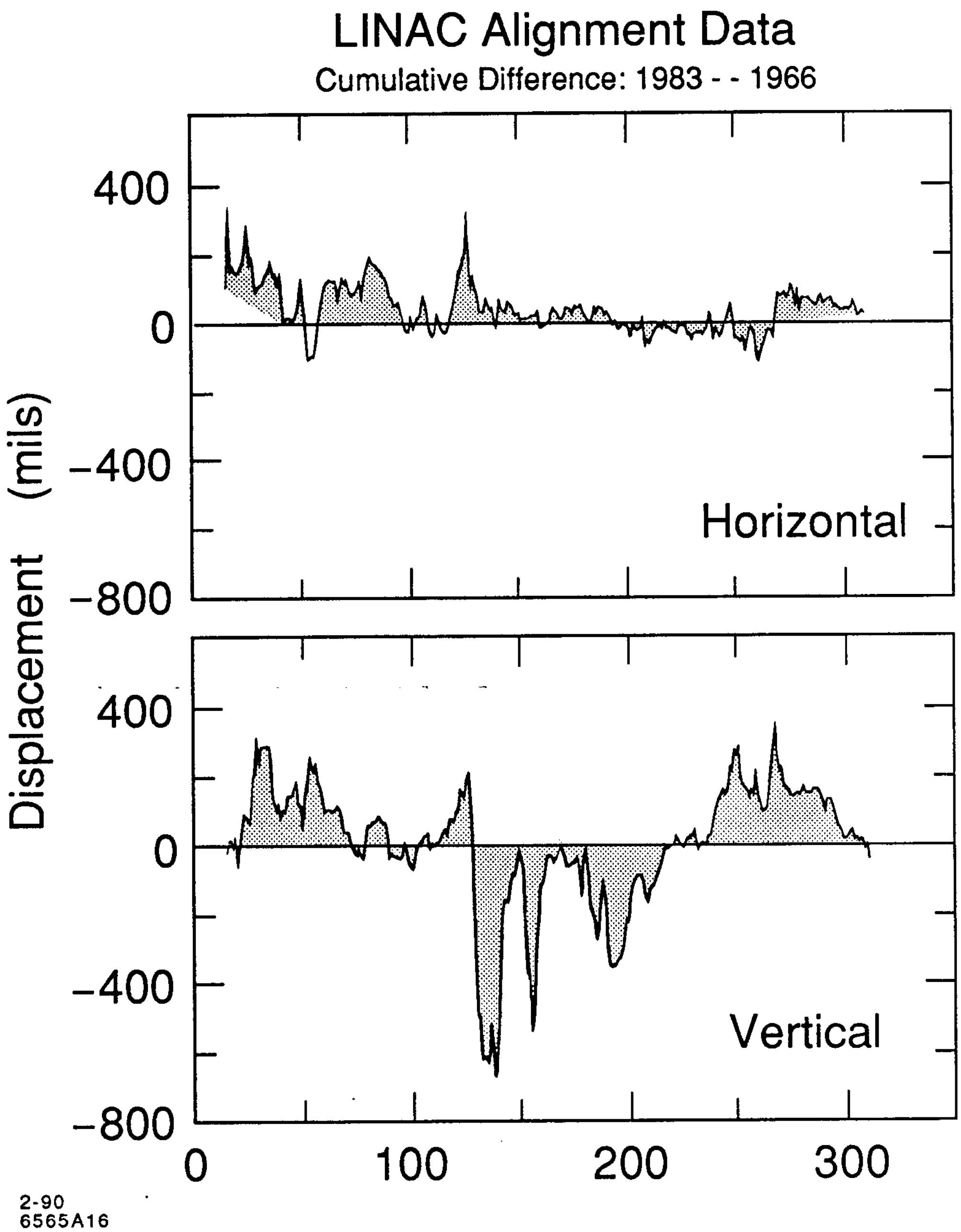
LINAC Alignment Data
Cumulative Difference: 1983 - - 1966
Displacement (mils)
400
0
−400
−800
Horizontal
Vertical
0
100
200
300
2-90
6565A16

Fig. 16

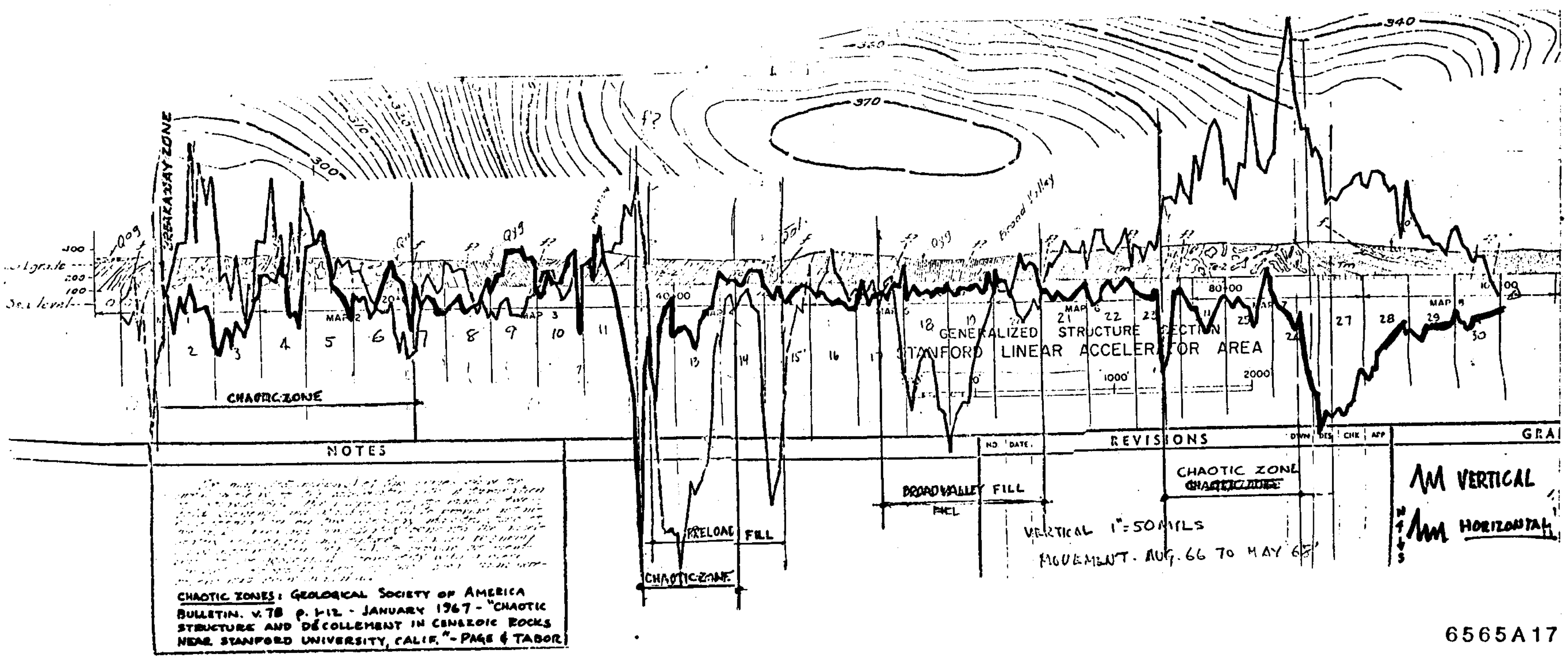

6565A17

Fig. 17

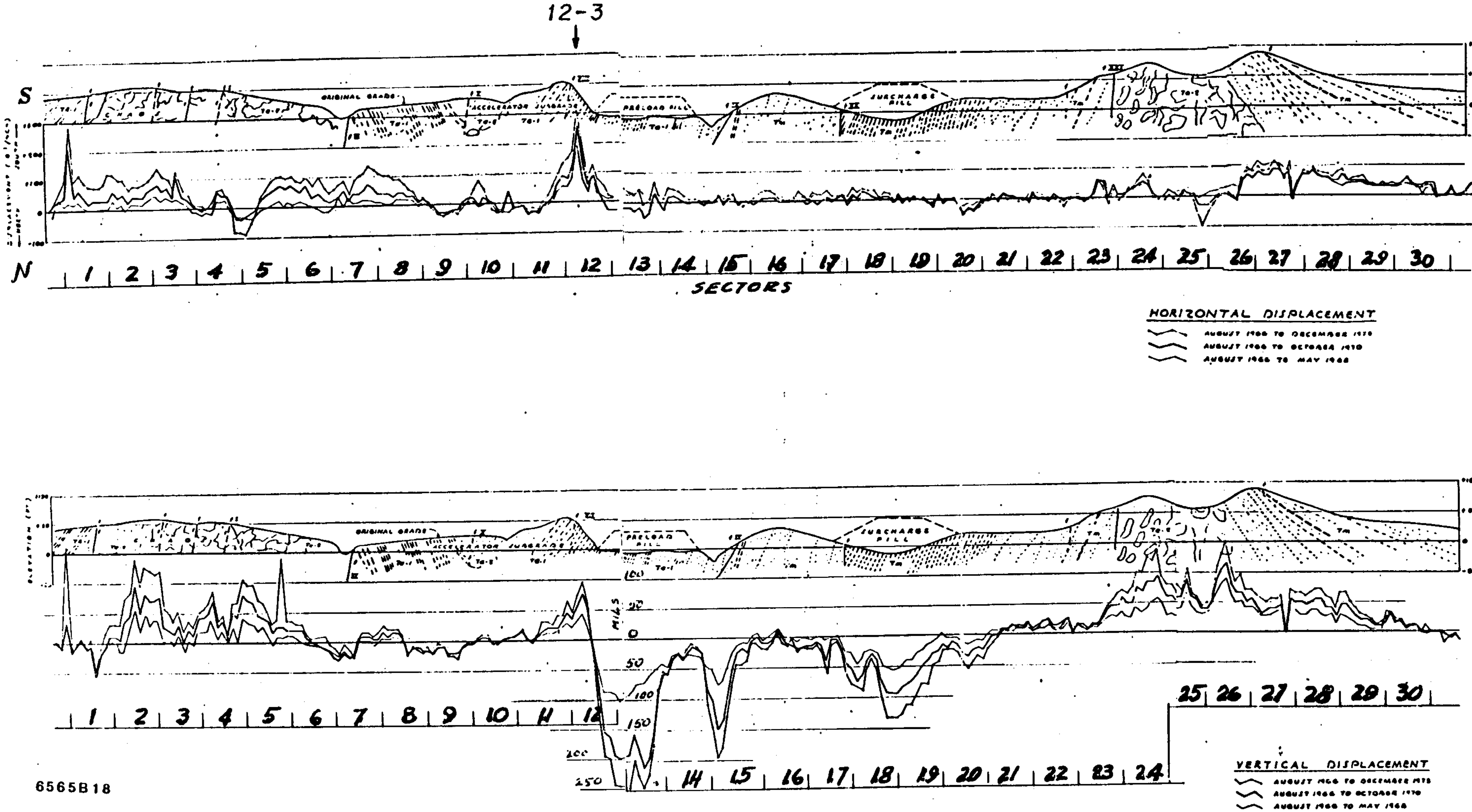

6565B18

Fig. 18

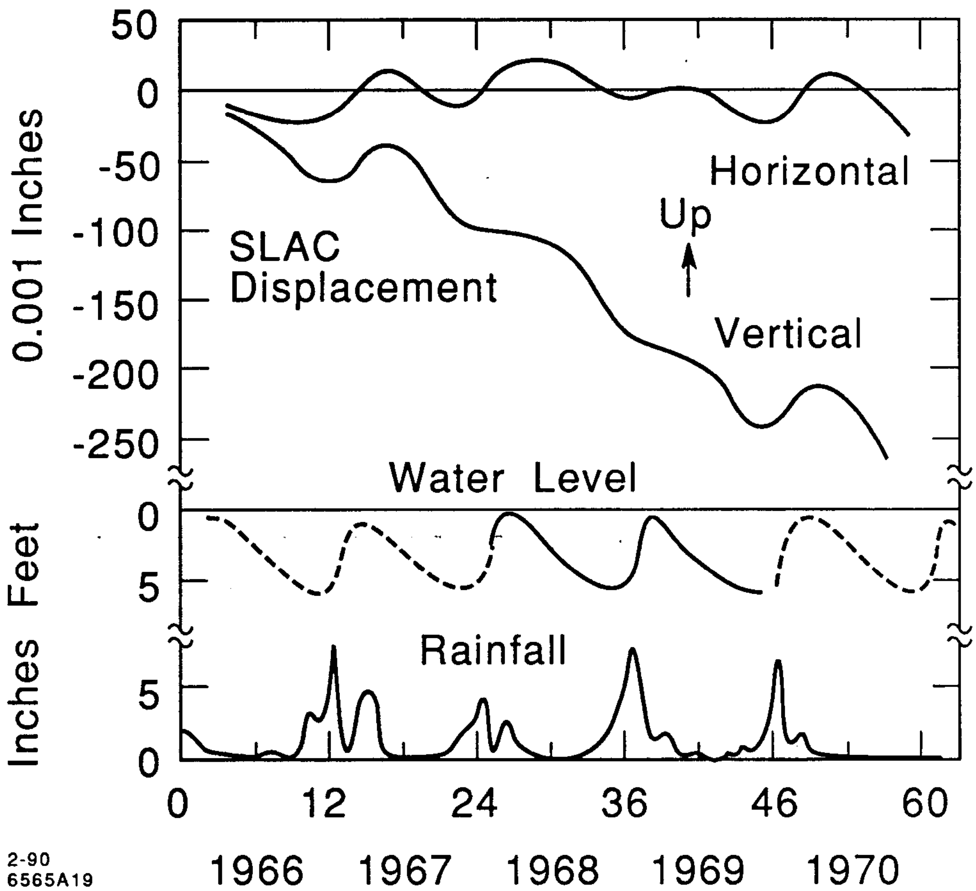
50
0
-50
-100
-150
-200
-250
0.001 Inches
SLAC
Displacement
Horizontal
Up
Vertical
Water Level
0
5
Feet
Rainfall
5
0
Inches
0
12
24
36
46
60
1966
1967
1968
1969
1970
2-90
6565A19

Fig. 19

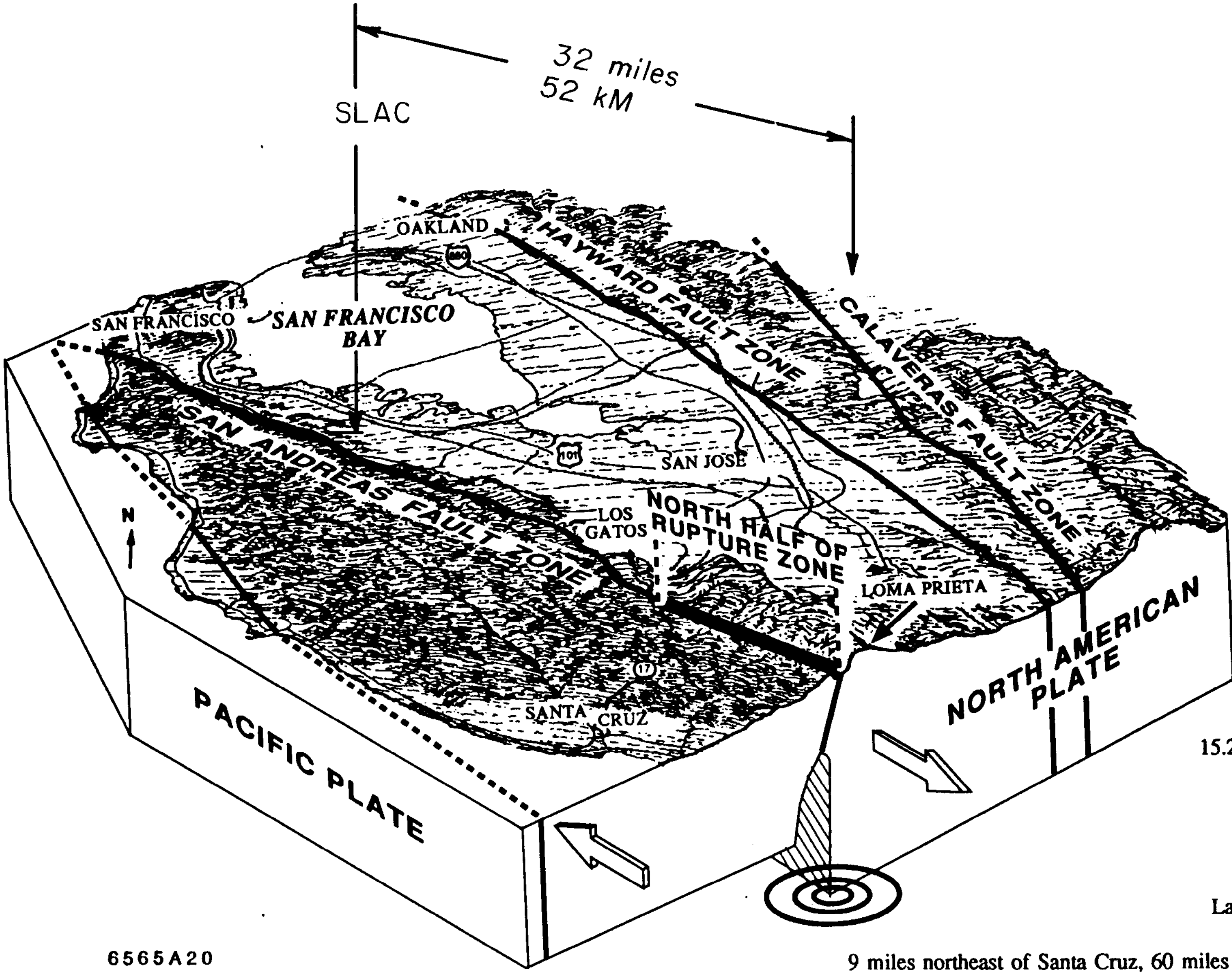

EARTHQUAKE ORIGIN

Time
October 17, 1989
15.24 seconds after 5:04 p.m. (PDT)

Magnitude
7.1

Location
Lat. 37.036° N., long. 121.883° W.
Depth 11.5 miles
9 miles northeast of Santa Cruz, 60 miles south-southeast of San Francisco

6565A20

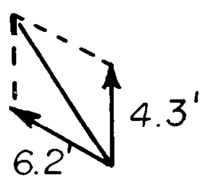

Fig. 20

Corrected Acceleration, Velocity, and Displacement at 200. SPS
Stanford University - SLAC Test Lab

Earthquake of Octorber 18, 1989 - 0004 GMT
Butterworth at 0.167 Hz Order 4

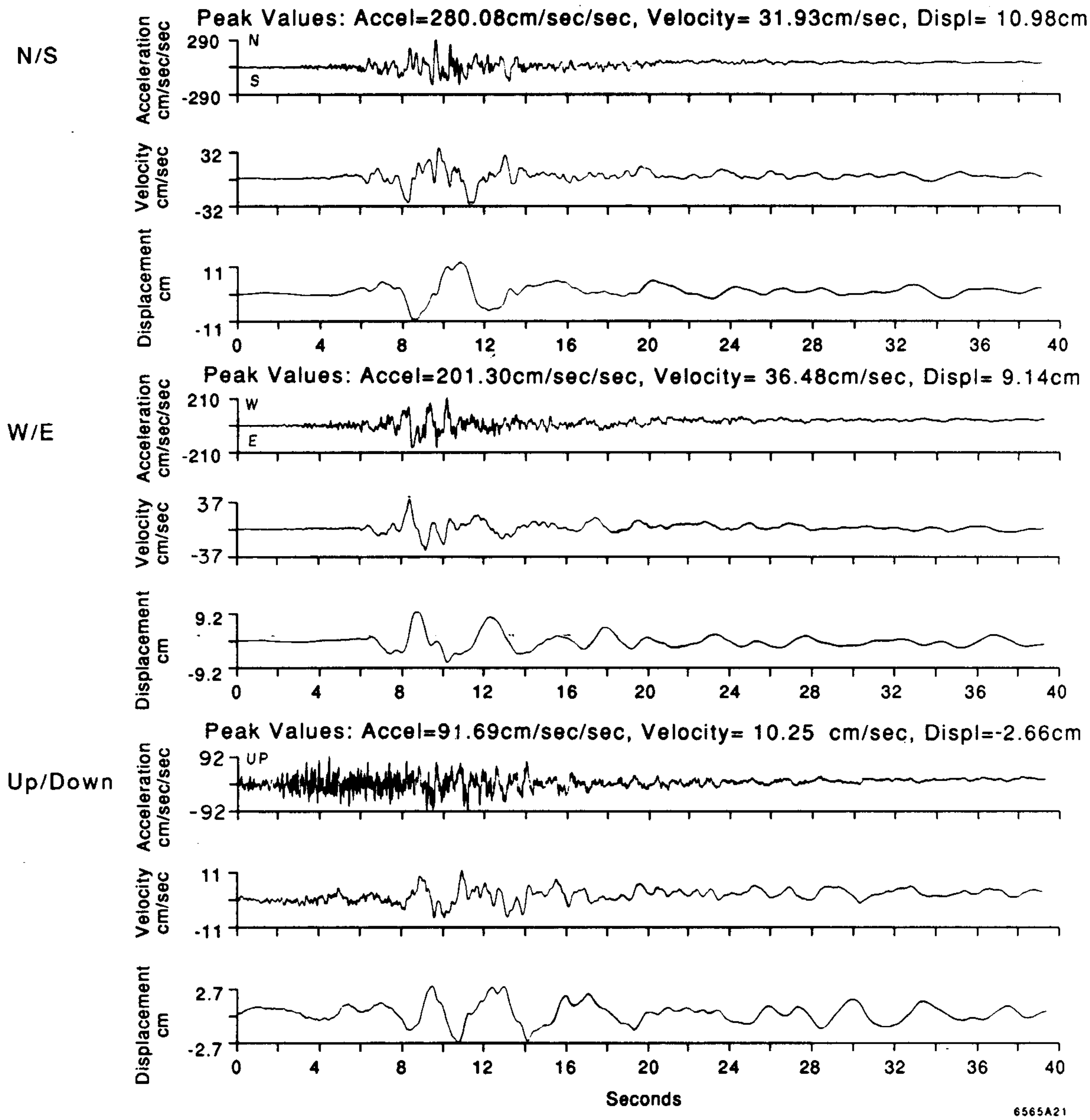

Fig. 21

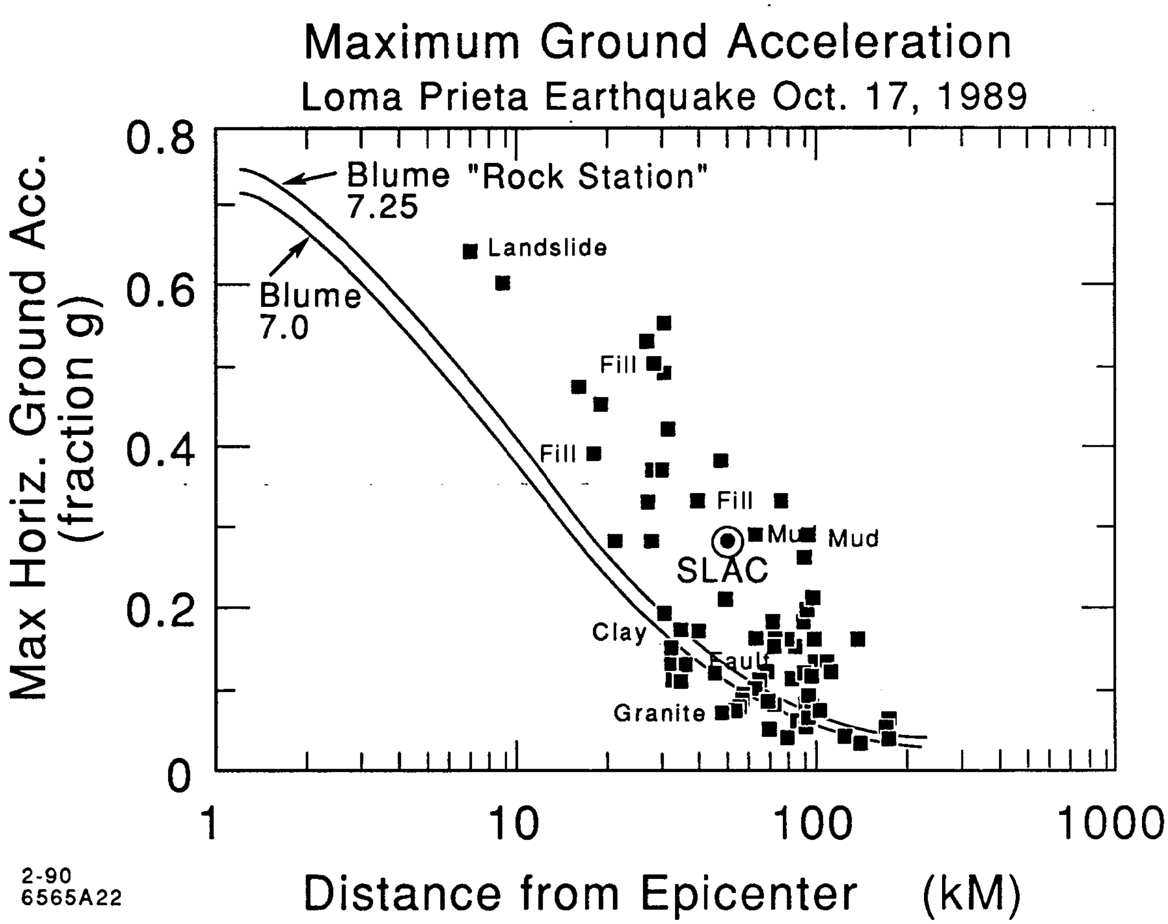
Maximum Ground Acceleration
Loma Prieta Earthquake Oct. 17, 1989
Max Horiz. Ground Acc. (fraction g)
0.8
0.6
0.4
0.2
0
1
10
100
1000
Distance from Epicenter (kM)
Blume "Rock Station" 7.25
Blume 7.0
Landslide
Fill
Fill
Fill
Mud
Mud
SLAC
Clay
Granite
2-90
6565A22

Fig. 22

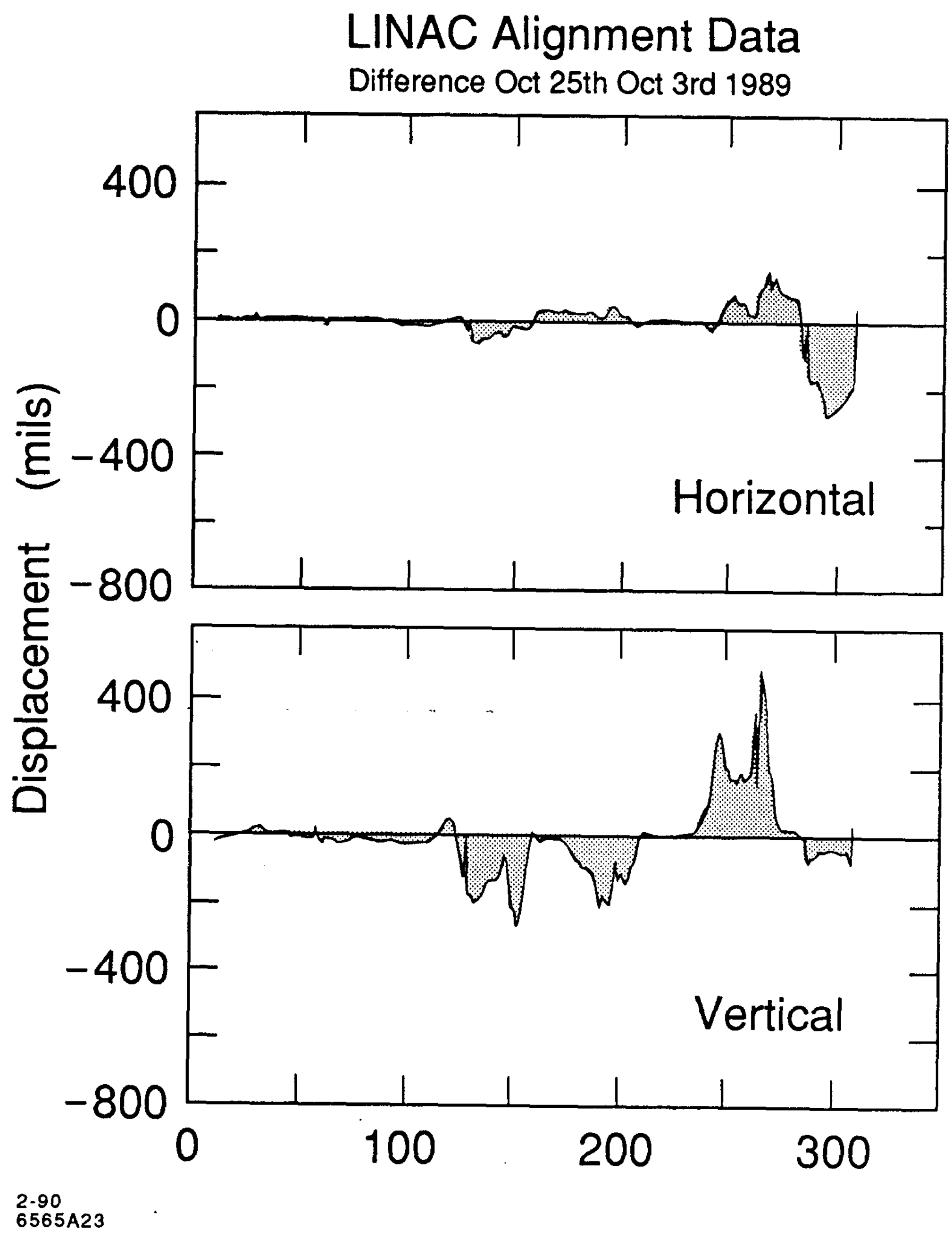
LINAC Alignment Data
Difference Oct 25th Oct 3rd 1989
400
0
-400
-800
Horizontal
400
0
-400
-800
Vertical
Displacement (mils)
0
100
200
300
2-90
6565A23

Fig. 23

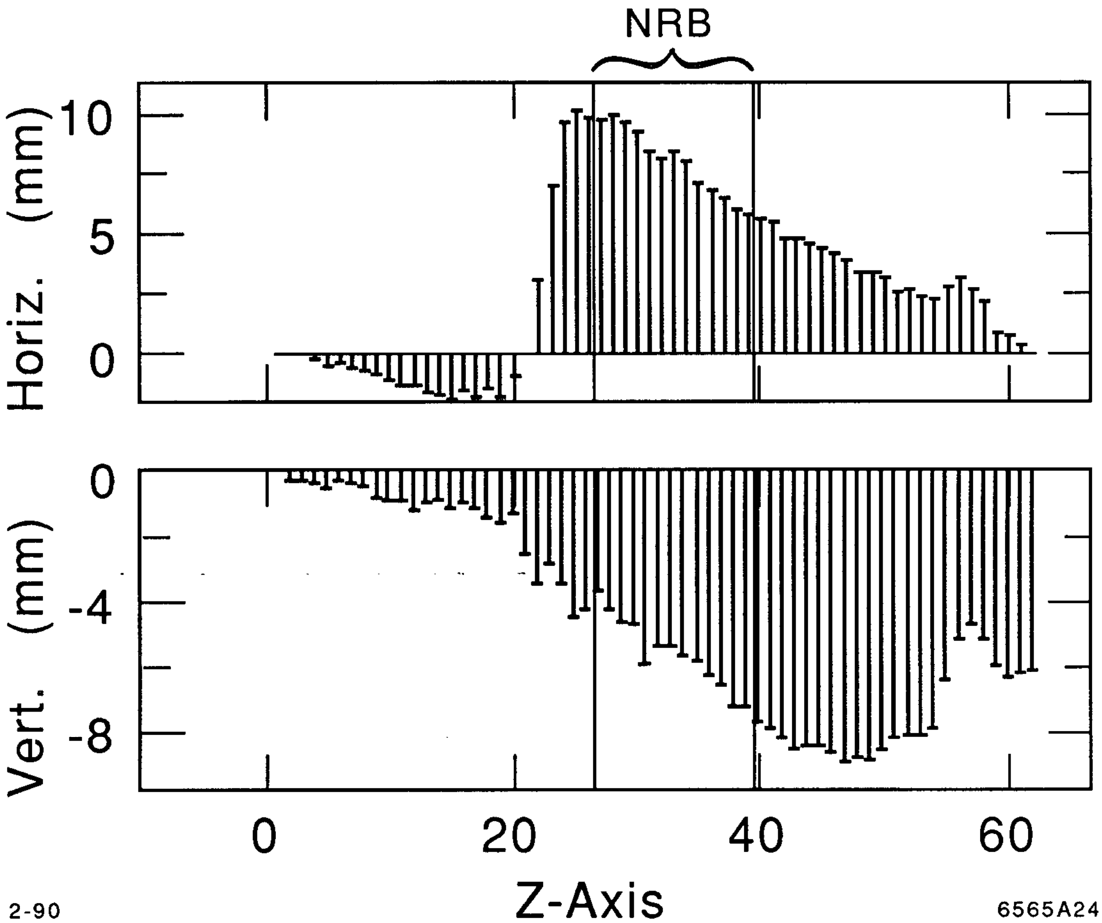

Fig. 24

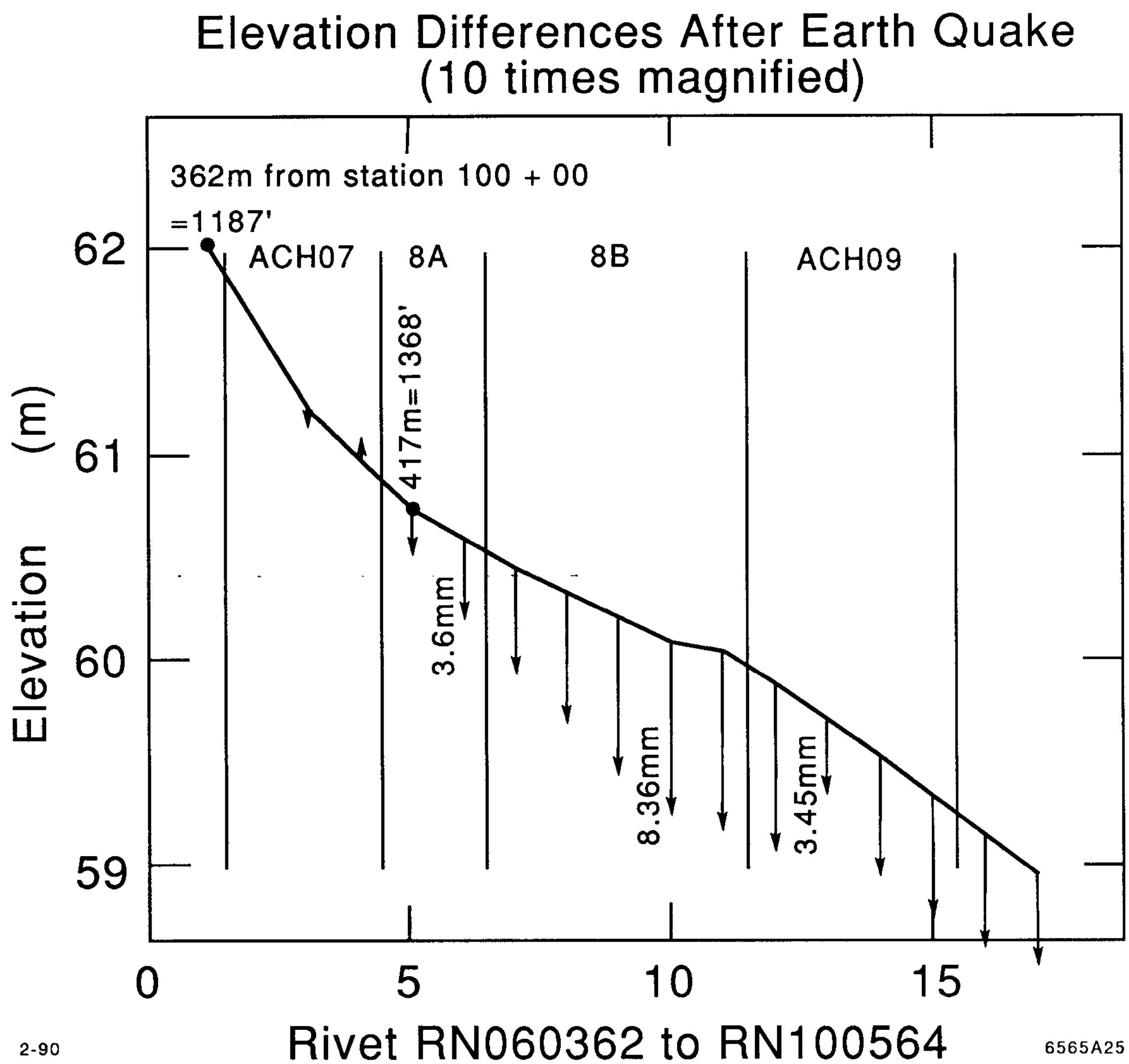
Elevation Differences After Earth Quake
(10 times magnified)
362m from station 100 + 00
=1187'
ACH07
8A
8B
ACH09
417m=1368'
3.6mm
8.36mm
3.45mm
62
61
60
59
Elevation (m)
0
5
10
15
2-90
Rivet RN060362 to RN100564
6565A25

Fig. 25

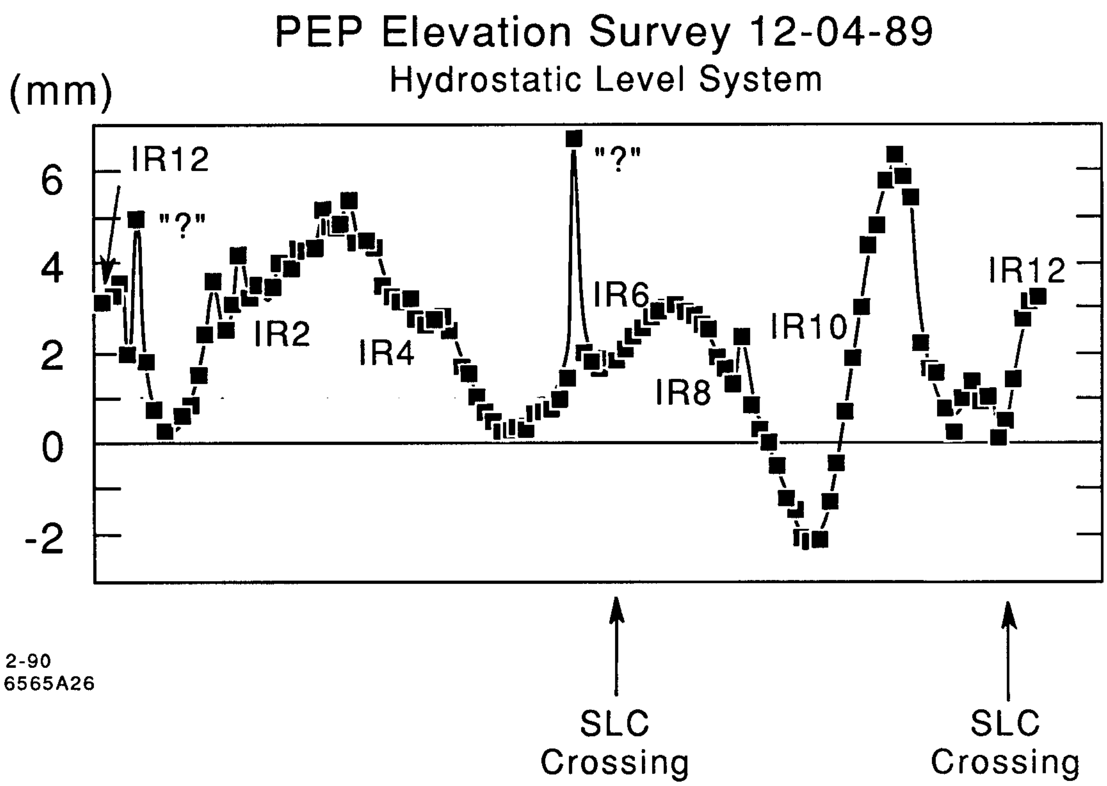

2-90
6565A26

Fig. 26

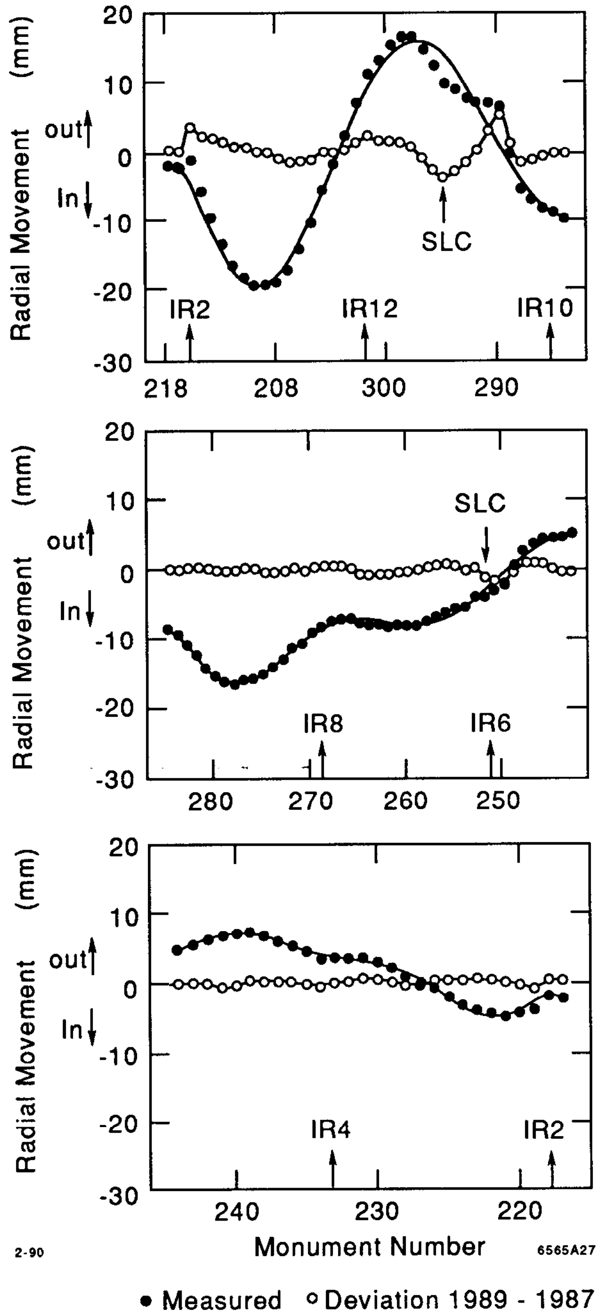

Radial Movement (mm)
out
In
20
10
0
-10
-20
-30
SLC
IR2
IR12
IR10
218
208
300
290
IR8
IR6
280
270
260
250
IR4
240
230
220
Monument Number
2-90
6565A27
• Measured ○ Deviation 1989 - 1987

Fig. 27

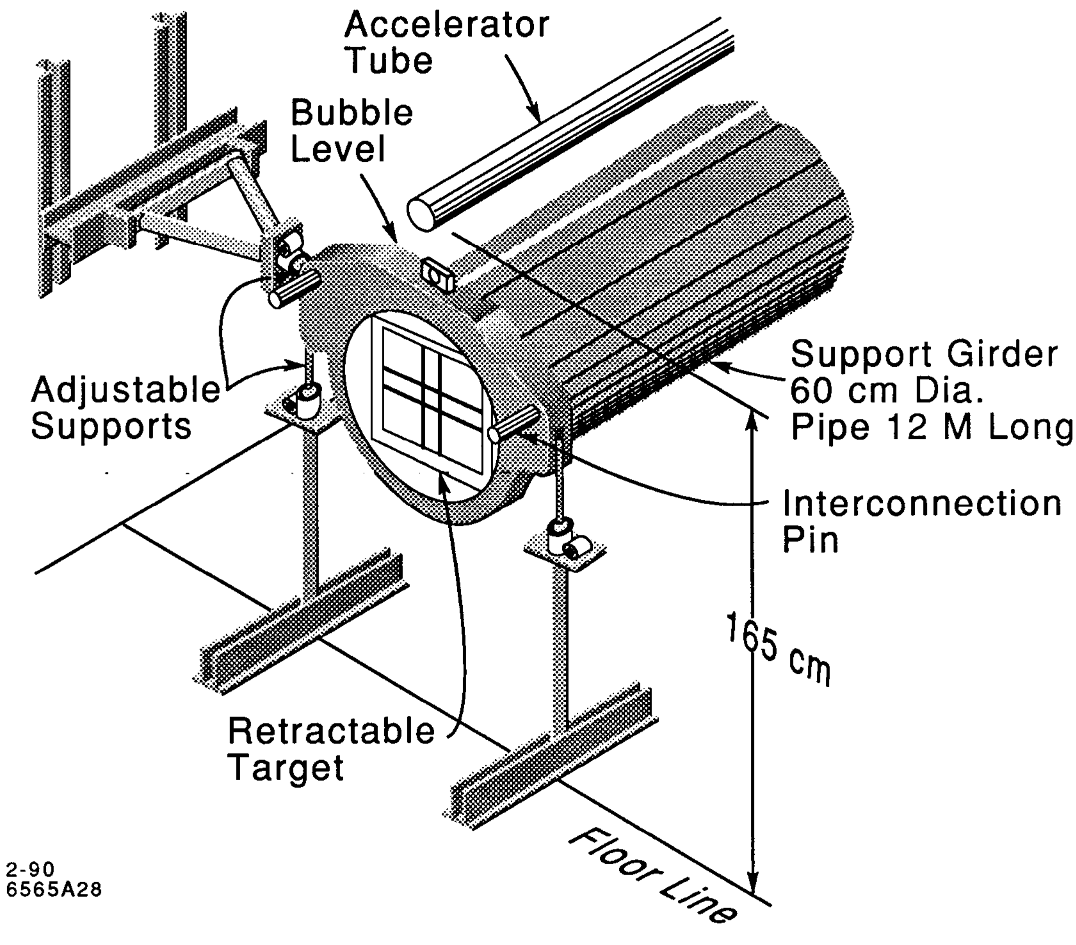
Accelerator
Tube
Bubble
Level
Adjustable
Supports
Support Girder
60 cm Dia.
Pipe 12 M Long
Interconnection
Pin
165 cm
Retractable
Target
Floor Line
2-90
6565A28

Fig. 28

Introduction

Base isolation is a design strategy founded on the premise that a structure can be substantially decoupled from damaging horizontal components of earthquake ground motion. This results in a significant reduction in the level of forces and accelerations to which the structure is subjected.

Use of the concept of base isolation has finally become a practical reality with the development of the lead-rubber bearing. Installed bearings exhibit flexible ductile behavior when subjected to severe earthquake motions and thus provide both dynamic decoupling and energy dissipation. The characteristics of a horizontally flexible mount, an energy dissipator and a vertical load support are contained within a single component.

Extensive research has confirmed the effectiveness and stability of lead-rubber bearings. Base isolation has emerged from the research environment to become a viable practical concept.

Lead-rubber bearings can be incorporated in the design of both new construction and the retrofit of existing structures. The bearings have already been used in a number of building and bridge structures in seismic areas. Base isolation incorporating lead-rubber bearings has been used in one new five-story building, fifteen new bridges and five existing bridges in New Zealand. They are also being used for the seismic retrofit of a bridge for the California Department of Transportation. The system is also

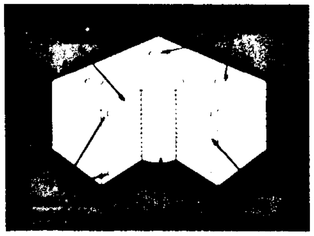

Figure 1

being considered for the design and retrofit of a number of buildings and other bridges in the United States.

Physical description

The physical construction of a typical lead-rubber bearing (see Figure 1) consists of the following components:

- Alternating rubber layers and thin steel plates are bonded together to form a unit having the desired stiffness properties of lateral flexibility and vertical rigidity.

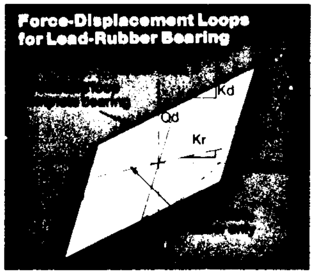

Figure 2

- A lead plug is tightly fitted into a preformed hole to provide both rigidity under low lateral load levels and energy dissipation under high loads.
- Top and bottom steel plates, substantially thicker than the interior plates, are designed to accommodate mounting hardware.
- Each bearing is encased in rubber to provide additional environmental protection.

The bearings are made in a wide range of sizes to accommodate diverse design requirements. They can be made in square, rectangular and circular plan shapes.

Behavior characteristics

When subjected to low lateral loads (such as minor earthquakes or wind), the lead-rubber bearing is stiff (vertically and horizontally) and remains elastic. The lateral rigidity results from the high elastic stiffness of the lead plug. The vertical rigidity (which remains at all load levels) results from the steel-rubber construction of the bearing.

At higher load levels, the lead yields and the lateral stiffness of the bearing is significantly reduced—this produces the period shift characteristic of base isolation concepts. It is important to note that the transition from low to high load levels is smooth; i.e., when the lead yields, additional load is carried primarily by the rubber but the load in the lead does not drop. This is a major advantage over other systems which rely on the failure of a wind restraint mechanism and the resulting sudden increase in load carried by the bearings.

Development

The lead-rubber bearing was the practical outgrowth of extensive research on base isolation performed in New Zealand. While the concept and advantages of base isolation have been understood for many years, research confirmed that base isolation would remain impractical without an energy dissipating mechanism to limit relative displacements between structure foundation and ground.

The lead plug fulfills this need. It provides an effective and economical means of providing energy dissipation. Moreover, it provides lateral rigidity to structures subjected to low lateral loads such as wind, minor earthquakes and braking forces (bridges).

Ductility

The benefits of ductility as an energy absorbing mechanism in earthquake-resistant design have long been recognized by the engineering profession. The lead-rubber bearings provide a means of incorporating ductility into a structure. The inelastic behavior is concentrated in a component specifically designed for this purpose. As a result, designers are given considerably greater latitude in the selection of architectural and structural forms. Nonductile systems previously discarded for aseismic design may once again become practical, economical and safe.

The seismic safety of existing nonductile construction can be considerably enhanced by the introduction of lead-rubber bearings to provide the necessary ductility.

Shaking table tests

In 1981, at the Earthquake Engineering Research Center, University of California, Berkeley, a series of shaking table tests were performed to evaluate the effectiveness of the lead-rubber system. The responses of a structure mounted on a fixed base were compared to those of a structure mounted on lead-rubber bearings. Using a 1/3-scale model of a five-story building, the effectiveness of the lead-rubber bearing system in providing base isolation and energy dissipation was demonstrated.

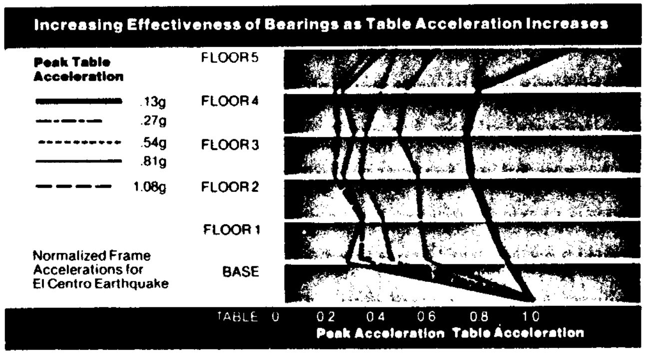

Figure 3

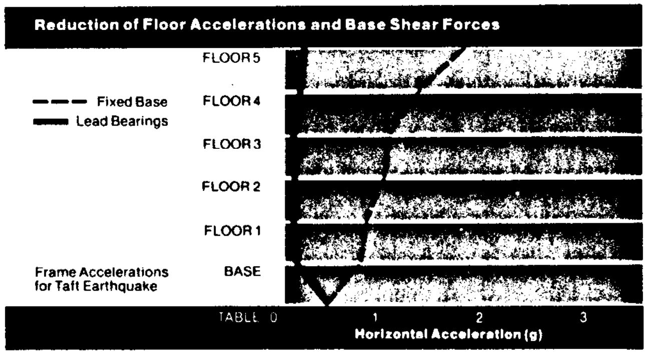

Figure 4

The following performance characteristics were confirmed:

(1) Floor accelerations were substantially reduced.

(2) Base shear and member design forces were significantly reduced.

(3) Interstory displacements were substantially reduced.

(4) The percentage reduction of accelerations increased with increasing earthquake magnitude.

These results are illustrated in Figures 3 and 4.

Additional shaking table tests are planned for the future. A series of tests on bridges incorporating lead-rubber bearings were performed in late 1983. These tests were sponsored by the The National Science Foundation.

Dynamic Isolation Systems, Inc.

The manufacture and use of the lead-rubber bearings is subject to patents in the United States and abroad. (U.S. Patent No. 4,117,637). For the United States, Canada and Mexico, the primary licensee is Dynamic Isolation Systems, Inc. (DIS) of Berkeley, California. DIS grants sublicenses to U.S. companies for manufacture and sale of the bearings.

The primary role of DIS is to promote the use of base isolation systems incorporating lead-rubber bearings. DIS develops design aids and procedures to assist engineers in the use of the system and works to gain code agencies' acceptance of the system and its accompanying design procedures. DIS sponsors research projects (such as shaking table testing) in order to gain further insight into the behavior and potential applications of the system. In addition, although DIS does not manufacture lead-rubber bearings, the firm constantly monitors manufacturing quality and performance specifications.

Consulting services on specific project applications are also available through DIS.

The Principals of DIS are Ronald L. Mayes and Lindsay R. Jones. Dr. Mayes, a graduate of the University of Auckland, has over eleven years' professional experience in earthquake engineering. He has been actively involved in several large-scale dynamic testing projects, as well as in developing seismic design guidelines for both bridges and buildings and was formerly the Executive Director of Applied Technology Council.

Dr. Jones, a graduate of the University of California, Berkeley, has over twelve years' professional experience in earthquake engineering. His specialization is in developing and applying computer analysis techniques to widely varied types of structures.

6565A29

Fig. 29

Mark II Positions

Post Earthquake

Relative to Pre-earthquake Monument Positions

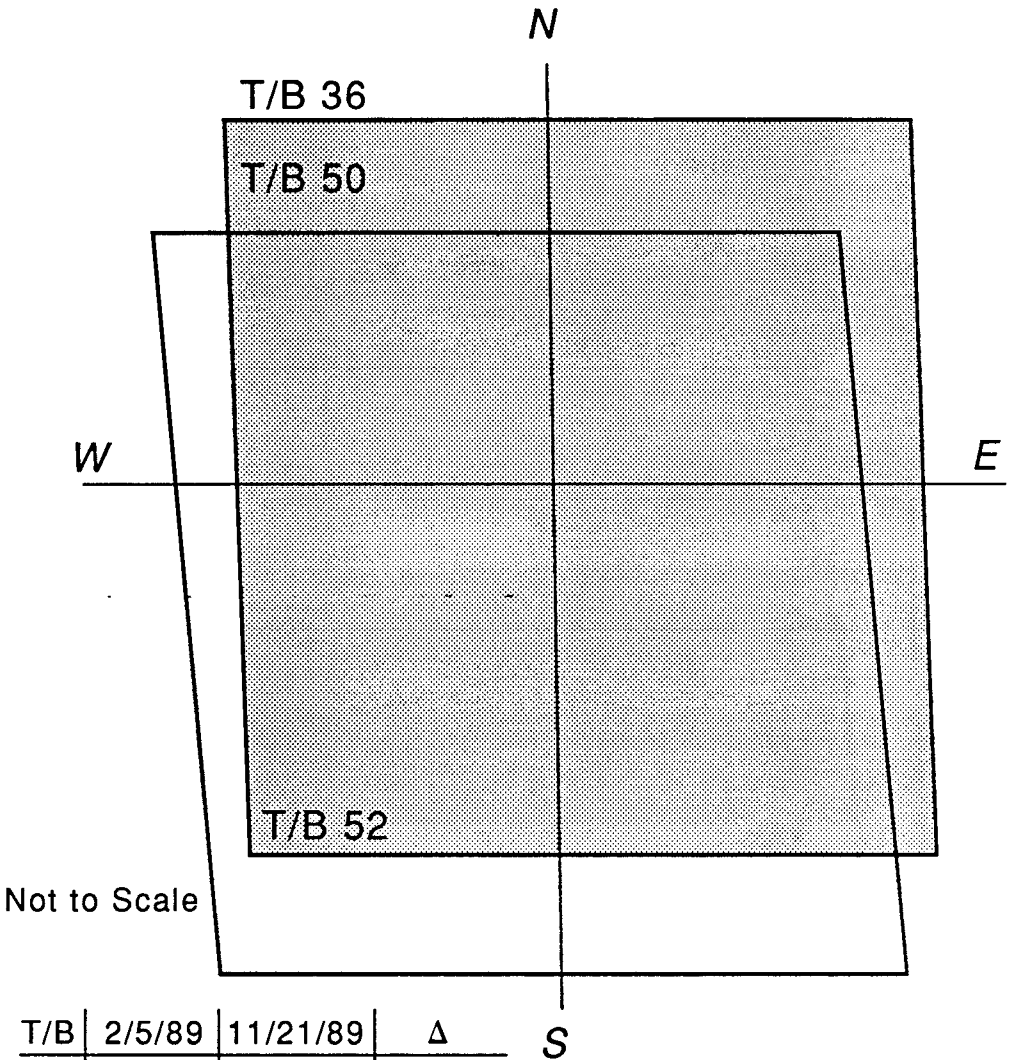

	T/B	2/5/89	11/21/89	Δ
X				
	50	0.047E	0.118W	0.165W
	52	0.067E	0.055W	0.122W
Z	36	0.087S	0.490S	0.403S

□ 11/21/89

▨ 2/5/89

2-90

6565A30

Fig. 30

APPENDIX A

THE BLACK MOUNTAIN ASPERITY: SEISMIC HAZARD OF THE SOUTHERN SAN FRANCISCO PENINSULA, CALIFORNIA

C. H. Scholz

Lamont-Doherty Geological Observatory and Department of Geological Sciences of Columbia University

Abstract. Black Mountain, a 860 m high wedge of Franciscan formation mostly comprising basic-ultrabasic rock SW of Palo Alto and just NE of the San Andreas fault, marks an abrupt bend in the fault at the northern end of a 100 km long segment of the fault that strikes 9° more E-W than the fault to the north or south. It also bounds a marked change in the physiographic setting of the fault, which to the north follows a well developed linear fault valley and to the south follows a poorly defined topographic trace that traverses the rugged Santa Cruz Mountains. The bend at Black Mountain had a profound effect on the 1906 rupture: the 75 km section to the SE of this point slipped only 1-1.4 m, as compared to the 2.5-4 m typical of the rupture on the San Francisco Peninsula to the NW. This 75 km long slip deficit region from Black Mountain to San Juan Bautista, if ruptured in its entirety would produce a M_S=6.9 earthquake: the conditional probability of this rupturing in the near future is the highest of any section of the San Andreas fault except Parkfield. This earthquake would rupture 30 km farther northwest and be about 3 times larger than that previously proposed by others and this constitutes a greater risk to the southern San Francisco Peninsula than previously expected.

Introduction

The role of asperities, geometrical irregularities such as bends and fault offsets, in affecting the faulting process has been extensively discussed in the recent seismological literature. Most recently, King and Nabelek [1985] have reviewed a number of cases in which fault bends have played a role in the initiation and inhibition of rupture. Here we review a particularly well documented case of this type. In the great California earthquake of 1906 the rupture propagated past an abrupt bend in the fault just adjacent to Palo Alto. At this point the NE side of the fault is bounded by an unusual topographic feature: a high ridge, subparallel to the fault, topped by the 860 m Black Mountain. Black Mountain is an ultramafic massif that lies in a wedge bounded by the San Andreas to the SW and the Black Mountain fault, which splays from the San Andreas at the northern end of the bend. This wedge, 3 kms wide at its SE edge, was found to be intensely shattered by the earthquake, and the slip on the main strand was reduced from 3 m just north of the bend to 1 m just south of it. This marks the northern end of the slip deficit section of the 1906 rupture that has been identified as one of the most likely sections of the San Andreas to rupture in a large earthquake in the near future [Lindh, 1983; Sykes and Nishenko, 1984; Scholz, 1985]. The finding that this zone extends to Black Mountain means that a potential rupture on this zone could propagate 30 kms farther to the NW than had previously been proposed and produce an earthquake with a seismic moment of about 3×10^{19} N-m, about three times larger than that proposed previously [Lindh, 1983; Sykes and Nishenko, 1984].

The 1906 Rupture

The southern part of the 1906 rupture zone of the San Andreas fault is shown in Figure 1. The rupture initiated off the Golden Gate (star, Figure 1 [Boore, 1977]) and propagated bilaterally over a distance of about 450 km. The southernmost 75 km of the rupture, from Black Mountain (BM) to San Juan Bautista (SJB) occurred on a segment that strikes about 9° more east-west than the fault to the north or south.

On the San Francisco Peninsula the rupture followed the linear fault valley defined by San Andreas Lake, Crystal Springs Reservoir, and Portola Valley. Offsets of numerous fences and pipelines generally indicate right lateral slip of 2.5-4 m in that region [Lawson, 1908]. North of the Golden Gate, slip was even greater, reaching 6 m in places. Fault offset data from Lawson (1908) for the region from Crystal Springs Reservoir south to San Juan Bautista is shown in Figure 2. Since all these measurements, which are of offset features such as roads and fences, are likely to underestimate the total slip, the most reliable data point that indicates a reduced slip for this section of fault is an offset of 1.4 m of a railroad tunnel at Wright. To the NW of Wright the slip reduction from 3 m to about 1 m occurs between Alpine Rd. and Page Mill Rd. (Figure 3). Alpine Rd. was apparently offset about 3 m, consistent with the data farther north (from an interpretation of Pl. 63A, [Lawson, 1908]). At Page Mill Rd. the fault lies in a trough with two strands about 10 m apart that cross the road at an angle of about 60° and produced two cracks which offset fences on both sides of the road about 0.9 m. The three data points between Wright and Page Mill Rd. are considered to be much less reliable but are consistent with reduced slip along this strand.

The slip reduction between Alpine Rd. and Page Mill Rd. corresponds precisely with the bend in the fault at Black Mountain (Figure 1). An enlarged view of that region is shown in Figure 3. The 9° bend of the fault occurs within the 5 km

C. H. Scholz, Lamont-Doherty Geological Observatory, Columbia University, Palisades, NY 10964

Paper number 5L6649.
0094-8276/85/005L-6649$03.00

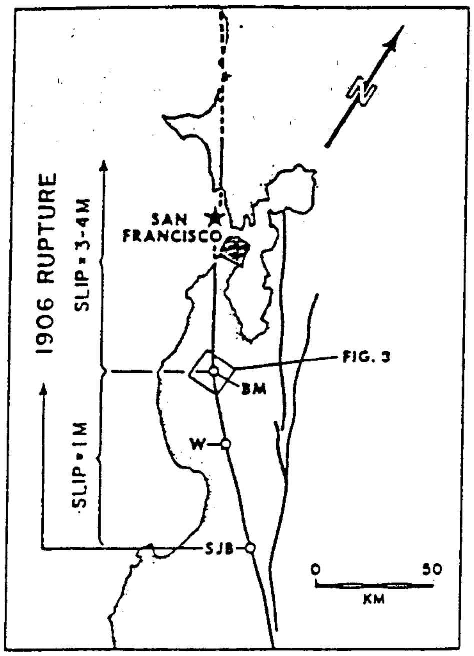

Fig. 1 Map of the southern part of the 1906 rupture on the San Andreas fault. The region discussed in the text is from Black Mountain (BM) through Wright (W) to San Juan Bautista (SJB). Star denotes epicenter of the 1906 earthquake.

segment between Alpine Rd. and Page Mill Rd. This bend occurs at a marked physiographic change in the fault where the fault leaves the well defined linear valley and to the SE follows a poorly defined trace that traverses the Santa Cruz Mountains. Two faults, the Pilarcitos fault and the Black Mtn. fault, splay symmetrically from the San Andreas fault on either side of the bend. The Pilarcitos fault is a strike-slip fault that is considered to be the ancestral San Andreas fault (J. Cummings, pers. comm., 1985) whereas the Black Mtn. fault is a thrust upon which the largely ultramafic mass of Black Mountain has been uplifted.

According to Branner's account in the Lawson report, just after the 1906 earthquake the first cracking encountered traveling to the SW up Portola Rd., Alpine Rd., and Page Mill Rd. was at the Black Mtn. fault, hence some minor coseismic slip may have occurred on this fault. The entire wedge between the Black Mtn. fault and the San Andreas fault was found to be extensively shattered. Page Mill Rd. was observed to be cracked in over 300 places between the two faults and the adjacent mountains were extensively cracked with no obvious correlation either with topography or with the strike of the San Andreas fault. This description of widely distributed crushing is unique among the faulting effects reported by Lawson [1908] and strongly suggests a connection between this, the bend, and the slip reduction at Black Mtn.

Since the Black Mtn. fault bend imposes a compressional restraint on fault slip, it is reasonable to suppose that the reduction in slip from 3 m to 1 m was caused by this bend and that the crushing of the wedge between the two faults in the interior corner of the bend is evidence of dissipation of the stress concentration that might be expected in such a situation [e.g. King and Nabelek, 1985]. This view is supported by the present existence of a cluster of microearthquake activity beneath Black Mtn. which exhibits focal mechanisms consistent with thrusting on the Black Mtn. fault and a compression direction nearly normal to the San Andreas fault [Olson, 1985]. A contrary view [Thatcher, 1975] that the slip reduction in 1906 corresponded with the northern end of the rupture of 1838 is not consistent with the data, since the 1838 rupture extended at least as far north as Woodside, and perhaps farther [Louderback, 1947], whereas the slip reduction occurred at Black Mtn., which is south of that point.

Expanding somewhat on King and Nabelek [1985] it is worth pointing out that the epicenter of the 1906 earthquake (Figure 1), although uncertain by ±20 km, apparently also occurs in a bend, inferred from the position of the fault landfalls on both sides of the Golden Gate. This bend, however, has the sense of implying release of right lateral slip, as opposed to the Black Mtn. bend, which implies an inhibition to slip. These cases are good examples of the two roles that fault bends can play in rupture, that of release and constriction of rupture.

Black Mountain and the Monte Bello Ridge are unusually high topographic features to the NE of the San Andreas fault. Black Mountain overthrusts Plio-Pleistocene gravels about 1-2 my old. The initiation of the uplift of Black Mtn. is approximately coincident with the abandonment of the Pilarcitos fault as the main strand of the San Andreas fault and is hence coincident with the creation of the fault bend [J. Cummings, pers. comm., 1985]. It seems likely, then, that the Black Mtn. asperity is a long-standing feature of the San Andreas fault and that Black Mtn. owes much of its topographic expression to uplift resulting from the compressional constraint imposed by the bend.

Seismic Hazard

A number of workers have estimated seismic hazard from earthquakes rupturing major seismic gaps of the San Andreas fault system [Lindh, 1983; Sykes and Nishenko, 1984; Scholz, 1985]. All have recognized the slip deficit region of the southern part of the 1906 break as being a

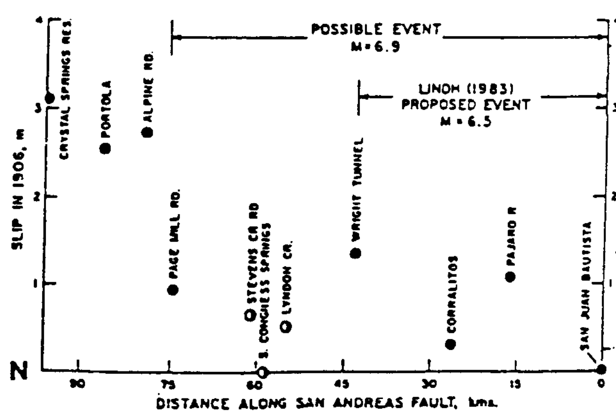

Fig. 2 Fault offset data for the 1906 earthquake: Crystal Springs to San Juan Bautista (from Lawson, 1908). Less reliable data are shown as half-filled circles.

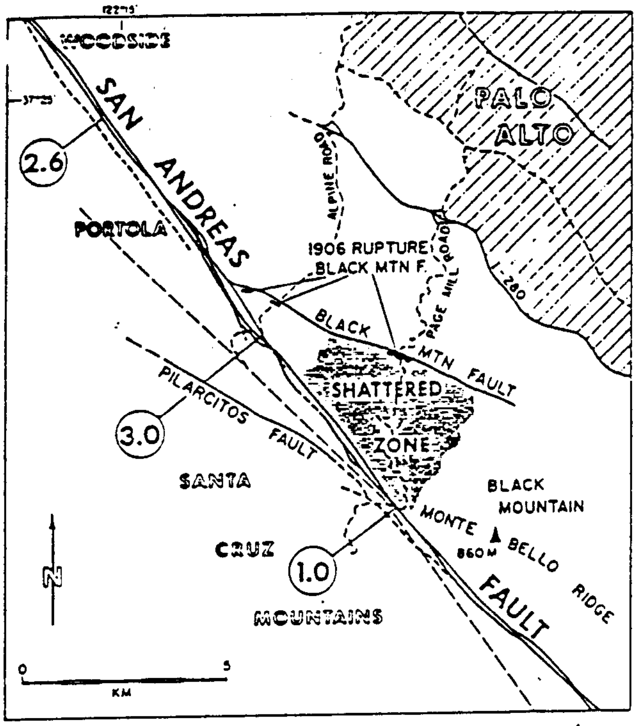

Fig. 3 Map of the region of the Black Mountain asperity, showing deformation and slip reported in 1906. Circled numbers are slip (in meters) reported in 1906.

likely site of a large earthquake in the next 20 years.

This segment was known to have ruptured in 1838, with slip occurring at least as far north as Woodside and possibly as far south as San Juan Bautista, since intensities reported at Monterey were higher (relative to 1906) than at San Francisco [Louderback, 1947]. Smaller earthquakes also occurred along or near this segment in 1865 and 1890. Thus this fault segment is known to slip on its own with a recurrence time as low as 68 years. Geologic estimates of the slip rate on this section are about 12 mm/yr [Hall, 1984] whereas geodetic data now indicate that the strain accumulation rate is 15 ± 2 mm/yr [Prescott et. al., 1985]. Thus if slip in 1906 was 1-1.4 meters, we can calculate that this strain would be re-accumulated in about 60-110 yrs: hence we infer that this region is now midway in a time window in which this fault segment may rupture. Sykes and Nishenko (1984), using similar data, estimated a conditional probability, with large uncertainties, of about 60% for this segment rupturing in the next 20 years. This is the highest estimate they made for any section of the San Andreas fault except Parkfield.

Lindh (1983), using an argument based on a change in geologic structure, suggested that the next earthquake would rupture between Wright and San Juan Bautista, a 45 km segment, in a M_s=6.5 earthquake. Although there is only one reliable data point (Page Mill Rd.) north of Wright that indicates that the region of slip deficit may extend considerably to the NW of Wright, the argument presented above supports the idea that the region of slip deficit extends from Black Mountain to San Juan Bautista since it provides a basis for suggesting that the slip at Page Mill Rd. is not a local aberration. This makes the segment that may rupture in a single earthquake about 75 kms long. Using a simple scaling relation for strike-slip earthquakes, $u=1.25\times10^{-5}L$ [Scholz, 1982], we can estimate that an earthquake rupturing this entire length would have the following parameters: $u=.9$ m, $M_o= 3\times10^{19}$ N-m, M_s=6.9. This earthquake is thus about 3 times larger in moment than the one predicted by Lindh [1983] and Sykes and Nishenko [1984] and poses a considerably greater risk since it would propagate adjacent to the highly developed Santa Clara Valley as far north as Palo Alto. The probability estimates they gave for the smaller earthquake would be the same for this larger event since the slip estimate for this event does not exceed that calculated to have accumulated since 1906.

Acknowledgments. I would like to thank A. Lindh, L. Sykes, J. Cummings, and K. Lajoie for useful discussions and W. Prescott for a preprint of his paper. This work was supported by NASA under grant NAG-5-446. Lamont-Doherty Geological Observatory Contribution Number 3879.

References

Boore, D.M., Strong motion recordings of the California earthquake of April 18, 1906, Bull. Seismol. Soc. Am., 67, 561-578, 1977.

Hall, N.T., Holocene history of the San Andreas fault between Crystal Springs Reservoir and San Andreas Dam, San Mateo Co., Calif., Bull. Seismol. Soc., Amer., 79, 281-299, 1984.

King, G.C.P. and J. Nabelek, Role of fault bends in the initiation and termination of earthquake rupture, Science, 228, 984-987, 1985.

Lawson, A.C., The California Earthquake of April 18, 1906 Carnegie Inst., Wash., D.C., 1908.

Lindh, A.G., Preliminary assessment of long-term probabilities for large earthquakes along selected segments of the San Andreas fault system in California, U.S. Geol. Surv. Open File Report, 83-63, 1-15, 1983.

Louderback, G.D., Central California earthquakes of the 1830's., Bull. Seismol. Soc. Am., 37, 33-74, 1947.

Olson, J. A., Seismicity of the San Andreas fault zone in the San Francisco Peninsula area, Proc. Int. Symp. Recent Crustal Movements, Wellington, New Zealand, in press, 1985.

Prescott, W.H., N.E. King, M. Lisowski, J.C. Savage, Deformation of the Pacific Plate Near San Francisco, California, Science, in press, 1985.

Scholz, C.H., Scaling laws for large earthquakes: consequences for physical models, Bull. Seismol. Soc. Am., 72, 1-14, 1982.

Scholz, C.H., Earthquake prediction and seismic hazard, Earthquake Pred. Res., 3, 11-25, 1985.

Sykes, L.R. and S. Nishenko, Probabilities of occurrence of large plate rupturing earthquakes for the San Andreas, San Jacinto, and Imperial Faults, California, 1983-2003, J. Geophys Res., 89, 5905-5927, 1984.

Thatcher, W., Strain accumulation and release mechanism of the 1906 earthquake, J. Geophys. Res., 80, 4862-4872, 1975.

(Received July 22, 1985; accepted August 15, 1985.)

APPENDIX B

MAXIMUM HORIZONTAL GROUND ACCELERATION VS. DISTANCE FROM SOURCE

For many years, workers at SLAC have been using curves for predicting maximum horizontal acceleration as a function of distance from the epicenter of a Northern California earthquake for stations located on Miocene strata as shown in figure B(1).

More recent work by Joyner and Boore (Ref. 28) suggests a formulation for the acceleration (y = fractional "g") as:

$$\log y = a + b(M-6) + c(M-6)^2 + d \log r + kr + s \quad .$$

in which $r = (r_o^2 + h^2)^{1/2}$, r_o is the shortest distance (km) from the recording site to the vertical projection of fault rupture on the surface, and M is the Richter magnitude. The parameters from fits to earthquakes of magnitudes greater than $M = 5$ in Western North America for the larger of the two horizontal components and for hypocenter depths less than 20 km are given to be: $a = 0.49$, $b = 0.23$, $c = 0$, $d = -1.0$, $k = -0.0027$, site correction for soil $s = 0$, and $h = 8$. This expression is plotted in figure B(2) as reported in the publication. When the vertical scale is made linear, the curves are as shown in figure B(3).

Although the Blume curves cannot be compared with the Joyner and Boore formulation at small distances, at 10 km they yield very similar accelerations, while at 100 km the Blume curves are a factor of two higher. The Blume curves seem to fit the data from the Loma Prieta earthquake quite well.

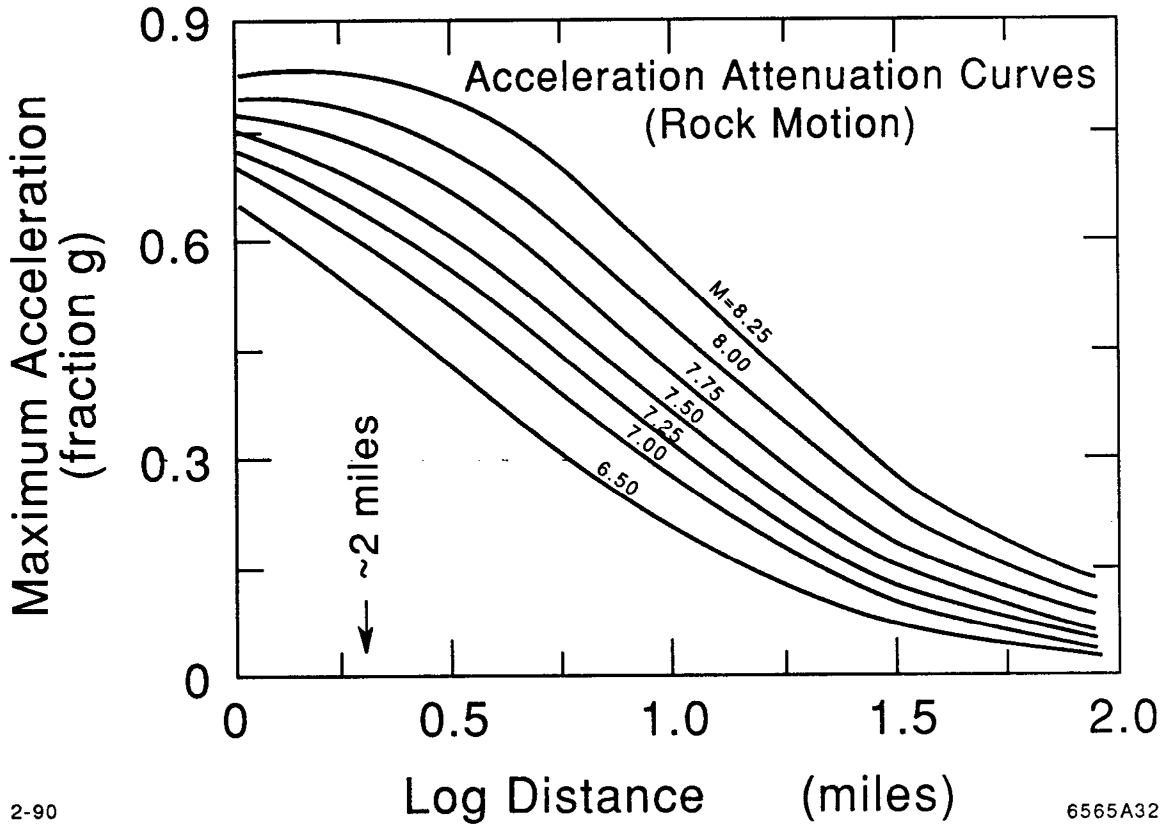

Acceleration Attenuation Curves
(Rock Motion)
Maximum Acceleration
(fraction g)
0.9
0.6
0.3
0
~2 miles
M=8.25
8.00
7.75
7.50
7.25
7.00
6.50
0
0.5
1.0
1.5
2.0
Log Distance (miles)
2-90
6565A32

Fig. B-1

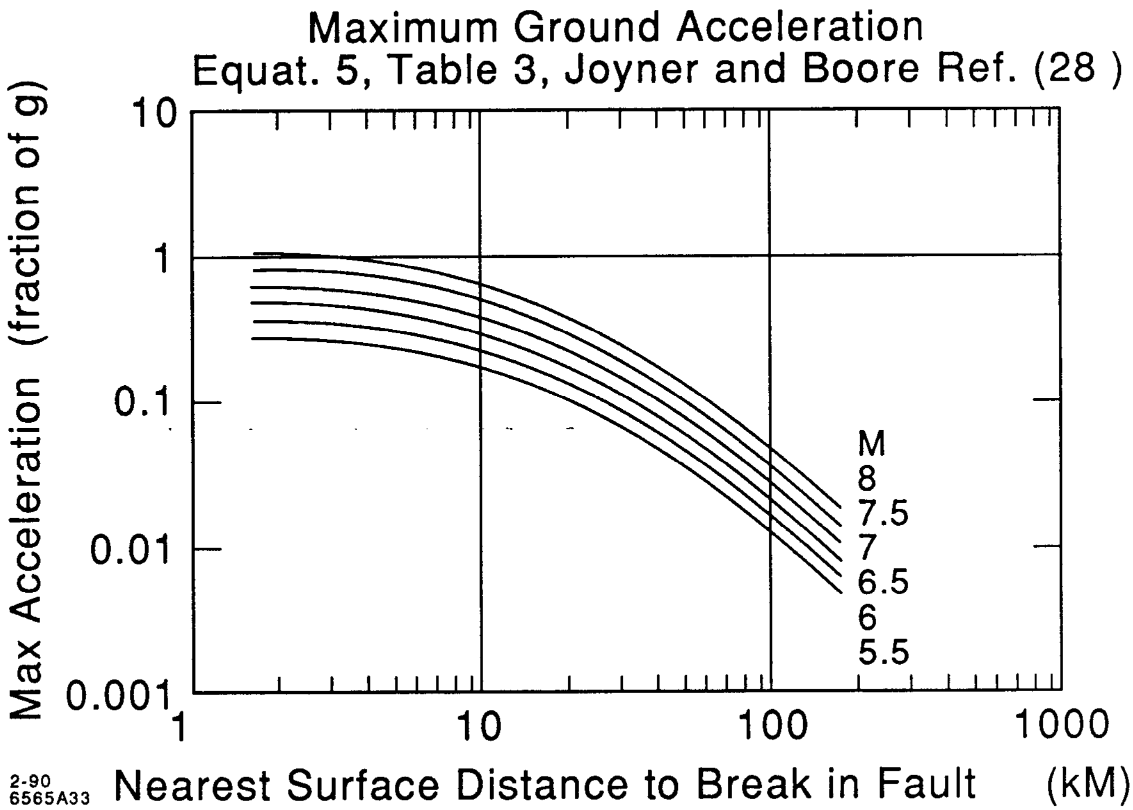
Maximum Ground Acceleration
Equat. 5, Table 3, Joyner and Boore Ref. (28)
Max Acceleration (fraction of g)
10
1
0.1
0.01
0.001
1
10
100
1000
M
8
7.5
7
6.5
6
5.5
2-90
6565A33
Nearest Surface Distance to Break in Fault (kM)

Fig. B-2